Chinese Journal of Structural Chemistry

REVIEW

Recent Progress in Covalent Organic Frameworks (COFs) for Electrocatalysis

Cha Li[1], Zining Qiu[1], Hongming Sun[1]*, Yijie Yang[1] and Cheng-Peng Li[1]*

[1]*College of Chemistry, Tianjin Key Laboratory of Structure and Performance for Functional Molecules, Tianjin Normal University, Tianjin 300387, China*

ABSTRACT Electrocatalysis provides various technologies for energy storage and conversion, which is an important part of realizing sustainable clean energy for the future. COFs, as emerging porous crystalline polymers, possess high specific surface areas, tunable pore structures, high crystallinity and tailorable functionalization. These features endow COFs with abundant active sites and fast electron transport channels, making them potentially efficient electrocatalysts. In recent years, COF-based electrocatalysts have been widely developed for hydrogen evolution reaction (HER), hydrogen oxidation reaction (HOR), oxygen evolution reaction (OER), oxygen reduction reaction (ORR), nitrogen reduction reaction (NRR) and carbon dioxide reduction reaction (CO_2RR). In this review, design strategies of COF-based electrocatalysts are briefly summarized, including applying COF as supports, introducing active metals in COF, constructing two-dimensional conductive COF, formation of COF-based hybrid and pyrolysis of COF to obtain carbon materials**.** Then, the recent research progress in COF-derived catalysts for specific electrocatalytic reactions is introduced systematically. Finally, the outlook and challenges of future applications of COFs in electrocatalysis are highlighted.

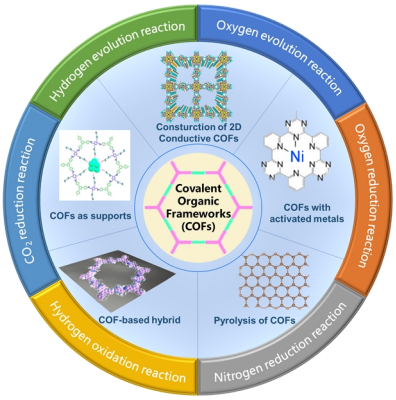

Keywords: covalent organic frameworks, electrocatalyst, catalytic performance, catalytic kinetics, energy conversion

n INTRODUNTION

The continuous consumption of fossil fuels results in gradually increasing energy shortage and environmental pollution problems, as well as the ever-present global climate problems. There is a growing need to explore fossil-free, sustainable, efficient and clean green energy sources.[1-3] Electrocatalysis is a practical chemical energy conversion process that converts atmospheric molecules (e.g., water, oxygen, nitrogen and carbon dioxide) into high chemical value products and fuels (e.g., hydrogen, oxygenates, ammonia, and hydrocarbons).[4] Electrocatalysts play a key role in this process, as they reduce the activation energy required for the reaction and increase the rate and selectivity of the reaction.[5] However, the current level of electrocatalysts is not yet adequate for large-scale commercial applications. Therefore, there is an urgent need to develop advanced electrocatalysts with high catalytic performance for these reactions.

In this regard, one of the prospective technologies is water splitting, which converts electrical energy generated from renewable energy sources such as solar and wind into chemical energy.[6-8] Water molecules decompose into hydrogen and oxygen when an additional voltage is applied to the electrode ($H_2O \rightarrow 1/2O_2 + H_2$). However, the bond energy between hydrogen and oxygen atoms is strong, which needs a lot of energy in thermodynamics to break.[9-11] According to the equilibrium potential E_θ of the electrochemical reaction and the formula: $\Delta G_\theta = - nFE_\theta$, the Gibbs free energy ΔG_θ for the water splitting reaction can be deduced. At 25 °C, the equilibrium potential E_θ of electrolyzed water is 1.23 V, so ΔG_θ is 237.2 kJ mol^{-1}, which is the minimum thermodynamically required energy value in the process of electrolysis of water[12]. In addition, the overpotential of HER, OER, and other resistors should be overcome. Hence, it is crucial to develop efficient catalysts to reduce energy consumption and speed up the water splitting reaction rate.

Up to now, noble metal platinum-based catalysts as well as ruthenium and iridium oxides are still high-efficiency benchmark catalysts in HER and OER,[13-16] respectively, but the scarcity, high cost, and poor stability hinder their extensive commercial application.[17] Researchers have developed various strategies to improve the intrinsic catalytic activity, conductivity and increase the catalytic active sites of electrocatalysts. Porous carbon materials have been widely used in electrocatalysis due to its large specific surface area, high electrical conductivity, good stability, sufficient active sites and low price.[18] However, the synthesis of most porous carbon materials requires pyrolysis, which is uncontrollable and also results in incomplete material skeleton. The increase of surface free energy can also lead to the inevitable aggregation of metal clusters or nanoparticles during pyrolysis.[19]

COFs, as crystalline porous polymeric materials with institutional building blocks connected by covalent bonds, have shown promising applications in gas/molecular capture/adsorption/storage, optoelectronic devices, heterogeneous catalysis, energy storage and sensing due to their high specific surface area, well-defined skeletons, highly ordered periodic structure and feasible functionalization.[20,21] After the first report of porous and crystalline COFs (COF-1 and COF-5) by Yaghi and co-workers in 2005,[22] COFs with various structural configurations have been reported.[23-25] COFs materials can be divided into 2D and 3D COFs according to their topological structures. COFs with different dimensions can be obtained by altering organic building

DOI: 10.14102/j.cnki.0254-5861.2022-0162

units, linkages and isoreticular expansion. In 2D COFs, monomers are connected by covalent bonds forming a layered structure in the plane, and the layers are conjugated through π-π interactions. One-dimensional channels are also formed in 2D COFs, and the size and shape of the channels are closely related to the stacking mode between layers. For 3D COFs, the monomers extend infinitely through covalent bonds, forming a framework with regular and periodic structures. Different from 2D COFs, 3D COFs are easy to form a large cage-like cavity, and the monomer can continue to react in the cavity and grow outward. Hence 3D COFs often get multiple interspersed structures.

Recently, COFs have been applied in several important electro- catalytic reactions including HER, hydrogen oxidation reaction (HOR), OER, oxygen reduction reaction (ORR), nitrogen reduction reaction (NRR), carbon dioxide reduction reaction (CO_2RR), etc.[26-30] To date, several groups have reviewed the development of COF-based electrolysts for some reactions including OER, ORR, HER, and CO_2RR.[31] However, the recent progress in COF-based electrolysts for HOR and NRR has not yet been summarized. Moreover, due to the rapidly increasing amount of reports on the COF-based electrolysts for these electrochemical reactions in the last two or three years, a timely review in this field is still needed. Here, we propose to summarize recent advances in the application of COFs in various electrocatalysis fields, focusing on their material design, role in catalytic reactions, active site engineering, catalytic performance, and mechanism. First, we briefly introduce the strategies for COF-based electrocatalyst design, such as using COFs as supports, introducing active metals into COF framework, constructing 2D conductive COF, complexing COF with active species and pyrolysis of COF to obtain carbon-based materials. Then, we summarize the applications and catalytic mechanisms of COF-based catalysts in various electrocatalytic reactions. Finally, we highlight the opportunities and challenges for developing COF-based electrocatalysts and provide perspectives for future research.

n DESIGN STRATEGIES FOR COF-BASED ELECTROCATALYSTS

COFs as Supports. Two basic design principles for improving electrocatalytic activity are to increase the number of active sites and to increase the intrinsic catalytic activity of each active site. Metal nanoparticles (e.g., Ni, Au, Ag, and Pt) have been widely used in electrocatalysis for various reactions due to their unique physicochemical properties. Meanwhile, based on the "quantum size effect", the size of nanoparticles directly affects their intrinsic properties.[32,33] With large surface area and high surface free energy, metal nanoparticles often exhibit excellent catalytic activity compared to their bulk counterparts. However, when the nanoparticles are very small, they tend to aggregate and fuse to form larger particles, leading to a decrease in their catalytic activity.[34] Therefore, to design and exploit high-performance and long-lasting catalysts, one valid strategy is to add supports for the active metal nanoparticles or nanoclusters, which not only avoids agglomeration of the loadings, but also facilitates the exposure of the active sites.[35] Unlike traditional metal oxides, COFs have well-defined frameworks, ordered structures, and ultrasmall pores that allow for uniform and controllable growth of nanoparticles within their frameworks. Meanwhile, COFs have a high specific surface area, which provides an opportunity to optimize the activity and stability of loaded nanomaterials for heterogeneous catalysis applications, making them strong candidates for new catalyst supports (Figure 1a).

COFs with Activated Metals. In general, transition metals have high stability, high electrical conductivity, and high activity for the electrocatalytic reaction.[36] Transition metal elements can be introduced into the framework of COF to improve the catalytic activity of COFs. Meanwhile, transition metal elements have empty *d* orbitals and high charge/radius ratios, which can easily form stable coordination compounds with various ligands by top-down, bottom-up or post-synthetic methods.[20]

For example, Yoon and coworkers designed Ir-modified tri-azine-linked COFs via post-synthetic immobilization method.[37] The prepared Ir-NHC-CTF showed an outstanding performance for the hydrogenation of CO_2 to formate. Kamiya and coworkers reported a metal-modified COF to photoelectrocatalyzing ORR.[38] Representatively, Yaghi and colleagues constructed metal-containing COF-366-Co and COF-367-Co/Cu by bottom-up method (Figure 1d), which condensed metalized porphyrin monomers with organic struts through imine bonds.[39] The active site of these electrocatalysts for CO_2RR is the Co/Cu metal of the porphyrin fraction. Hence, adding tunable molecular units can controllably synthesize COF-based electrocatalysts with activated metals, which will be suitable for a wide range of catalytic applications, especially in heterogeneous catalysis that requires metal participation.

Construct of Two-Dimensional Conductive COFs. Generally, precise controlling the electrical conductivity of an electrocatalyst has been pursued to achieve enhanced catalytic performance. An effective strategy to realize the optimization of COFs's conductivity is exfoliating bulk COFs to form single or few layers 2D polymers in planar conformations, which can improve the accessibility of active sites (Figure 1c). Meanwhile, the stacked form of 2D material can reduce the recombination energy and enhance the coupling between π electrons, thus realizing interlayer electron conduction perpendicular to the layers. Fang and coworkers delaminated porphyrin-based mesoporous 2D COF composed of a capacitor cell, which exhibited excellent charge storage capacity at high scan rate.[40] In 2021, Bhaumik et al. reported a thin two-dimensional triazine-based C_6-TRZ-TFP COF by condensing 2-hydroxybenzene 1,3,5-tricarboxaldehyde (TFP) and 4,4',4"-(1,3,5-triazine-2,4,6-triyl)tris([1,1-biphenyl]-4-amine), which exhibited excellent electrocatalytic HER performance with an overpotential of 200 mV at a current density of 10 mA cm^{-2}, outperforming most of the reported metal-free COFs as well as triazine-based COFs.[41] In 2022, an olefin-linked 2D COF was prepared using nanographene and dibenzo[hi,st]ovalene (DBOV) as a building block by Narita et al.[42] As-prepared DBOV-COF possessed high crystallinity, stability with high charge mobility and exhibited high photocatalytic properties.

Chin. J. Struct. Chem. **2022**, 41, 2211084-2211099
DOI: 10.14102/j.cnki.0254-5861.2022-0162

COF-Based Hybrids. Controlled synthesis of COF-based hybrids is also an effective strategy to achieve excellent catalytic performance (Figure 1d). The complexed species coupled with COF include organic polymers (such as polyaniline,[43] etc.), carbon-based materials (such as graphene,[44] carbon nanotubes,[45] etc.), inorganic species (such as polysulfide,[46] etc.), Zeolitic Imidazolate Frameworks (ZIFs),[47] and Metal Organic Frameworks (MOFs).[48] For example, Du et al. reviewed MOF/COF-based hybrid nanomaterials with large specific surface area, small band gap, and large pores, which are beneficial for researchers to expand the application of COF-based hybrids.[48] In addition, if COF is compounded with a conductive substrate material, its electron transport capacity can be enhanced, thus improving the specific catalytic properties of the hybrids.

Pyrolysis of COF to Obtain Carbon-Based Materials. Carbon-based materials are one of the most commonly used materials in the field of electrocatalysis because of their high electrical conductivity and stability, as well as large surface area and pore volume. Many organic precursors have been used to synthesize carbon-based materials due to their ability to introduce heteroatoms and easy formation of high surface area materials. COFs are suitable candidates for heteroatom-doped carbon precursors because they are heteroatom- and carbon-rich (Figure 1e). Furthermore, the periodic character of COFs with dispersed metal coordination sites may yield the final carbon materials with single atom. Based on the above properties, COFs are promising precursors for preparing carbon materials. For example, in 2019, Thomas et al. obtained iron-nitrogen doped mesoporous carbon (mC-TpBpy-Fe) by carbonizing COF precursors at a high temperature of 800 °C, which showed high ORR catalytic performance.

n COF-BASED ELECTROCATALYSTS FOR HYDROGEN EVOLUTION REACTION AND HYDROGEN OXIDATION REACTION

Hydrogen energy has attracted extensive attention due to its high efficiency, cleanliness, and renewable characteristics, and is also considered as one of the sustainable alternative energy sources to solve the current environmental pollution and energy crisis.[49] Renewable hydrogen (H_2) technologies including HER and HOR are operated in various highly efficient electrochemical processes, such as electrolysis of water and H_2 fuel cell. Currently, hydroxide-exchange-membrane water electrolyzer (HEMWE) and hydroxide-exchange-membrane fuel cells (HEMFC) have attracted

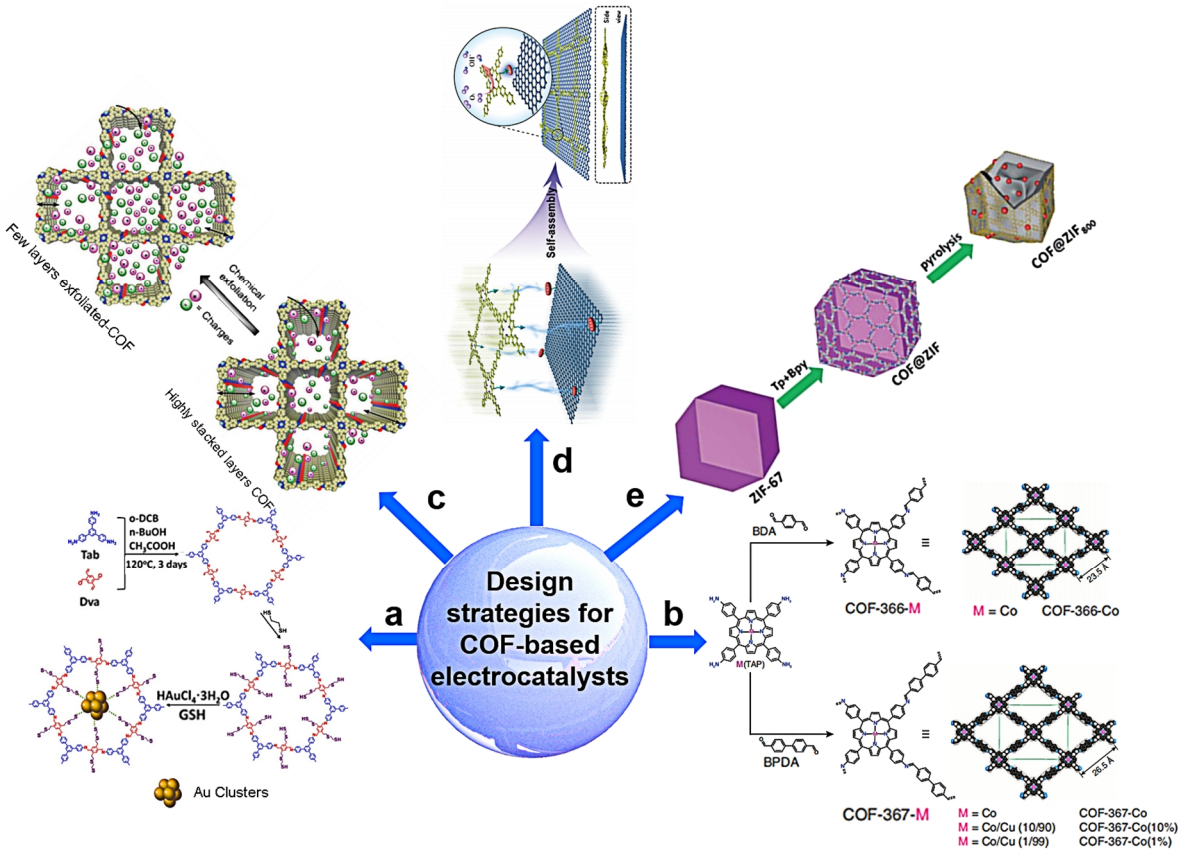

Figure 1. General design strategies for COF-based electrocatalysts. (a) COFs as supports.[34] Copyright 2020 Wilry-VCH. (b) COFs with activated metals.[39] Copyright 2015 American Association for the Advancement of Science. (c) Construction of two-dimensional conductive COF nanosheets.[40] Copyright 2020 American Chemical Society. (d) COF-based hybrids.[44] Copyright 2018 Wiley-VCH. (e) Pyrolysis of COF to obtain carbon-based materials.[47] Copyright 2022 Royal Society of Chemistry.

DOI: 10.14102/j.cnki.0254-5861.2022-0162

enormous attention.[50,51] A main reason is that abundant and inexpensive catalysts can replace platinum-based metals to catalyze the ORR and OER, which significantly reduces the cost of fuel cells and water electrolyzers. This promotes them as promising alternatives for proton-exchange-membrane electrolyzers and proton-exchange-membrane fuel cells. However, the lack of efficient, low-cost and stable electrocatalysts for HER and HOR hinders the commercialization of HEMWE and HEMFC. Up to now, platinum-based catalysts are still the best HER/HOR catalysts, but their large-scale commercial application is hindered by the scarcity of platinum resources, high cost, and poor stability.[52]

Hydrogen Evolution Reaction: The reaction processes of hydrogen evolution reaction in alkaline and acidic medium are as follows:

Alkaline:

Volmer step: $H_2O + M + e^- \rightarrow MH_{ads} + OH^-$ (1)

Heyrovsky step: $MH_{ads} + H_2O + e^- \rightarrow M + OH^- + H_2$ (2)

Tafel step: $2MH_{ads} \rightarrow 2M + H_2$ (3)

Acidic:

Volmer step: $H^+ + M + e^- \rightarrow MH_{ads}$ (4)

Heyrovsky step: $MH_{ads} + H^+ + e^- \rightarrow M + H_2$ (5)

Tafel step: $2MH_{ads} \rightarrow 2M + H_2$ (6)

Compared with the cleavage of H-O-H bonds under alkaline conditions, the adsorption of hydrated protons (H_3O^+) in the Volmer step of HER under acidic conditions is easier, so it is favorable for HER to proceed under acidic conditions. Meanwhile, regardless of medium, the Volmer process must be experienced. When the Volmer process is fast and the Tafel step is a fast-controlled step, the Tafel slope of HER is less than 30 mV dec^{-1}; when the Volmer step is fast and the Heyrovsky process is a step-controlled step, the Tafel slope of HER is 30-40 mV dec^{-1}; when the first step of HER (Volmer reaction) is relatively slow, the Tafel slope of the reaction is larger than 120 mV dec^{-1}.

Furthermore, the adsorption and desorption processes of H are involved in the reaction process, so the free energy of hydrogen adsorption and desorption (ΔG_{H^*}) is usually used as a descriptor for the performance of HER catalysts.[53] According to literature reports,[54] there is a volcano-like relationship between ΔG_{H^*} and the exchange current density j_0. The ΔG_{H^*} of the Pt catalyst is close to zero and has a large exchange current density, so it is the best HER catalyst. Therefore, the designed electrocatalyst should have a ΔG_{H^*} close to zero.

The emergence of COFs provides a new platform for designing novel HER electrocatalysts. Bhunia and colleagues were the first to report crystalline two-dimensional COFs (SB-PORPy) for electrochemical hydrogen production.[28] The COF was prepared by a solvothermal method using 5,10,15,20-tetrakis(4-aminophenyl) porphyrin (TAP) and 1,3,6,8-tetrakis(4-formylphenyl) pyrene (TFFPy) as raw material (Figure 2a, b). The resulting COF has a specific surface area of 869 m^2 g^{-1}. The synthesize COF and carbon black were milled at a weight ratio of 1:1. In 0.5

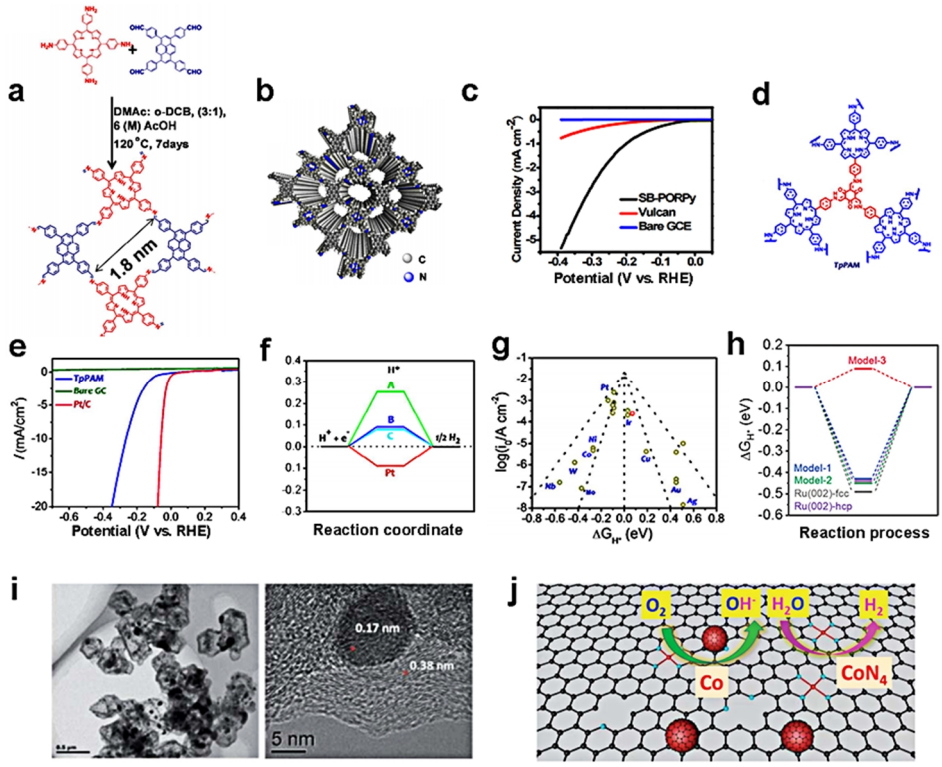

Figure 2. COF-based HER electrocatalyst. (a) Schematic of SB-PORPy COF. (b) Top view of AA stacking SB-PORPy COF. (c) HER polarization curve of SB-PORPy COF.[30] Copyright 2017 American Chemical Society. (d) Schematic of TpPAM. (e) HER polarization curves of TpPAM. (f) Free energy diagram for HER on the investigated four catalysts. (g) The volcano plot of the $\log i_0$ versus ΔG_{H^*} of Model C and transition metal catalyst.[55] Copyright 2017 American Chemical Society. (h) Calculated ΔG_{H^*} for the several models.[57] Copyright 2022 Wiley-VCH. (i) TEM and HRTEM images of COF@ZIF_{800}. (j) The catalytic mechanism of COF@ZIF_{800} for ORR and HER.[47] Copyright 2022 Royal Society of Chemistry.

DOI: 10.14102/j.cnki.0254-5861.2022-0162

Table 1. List of Some Reported COF-Based Electrocatalysts for HER and Their Experimental Catalytic Activities

HER electrocatalysts	Overpotential (mV)	Tafel slope (mV dec^{-1})	Electrolyte	Ref.
CoP-2ph-CMP-800	360 mV at 10 mA cm^{-2}	121	1.0 M KOH	61
2DCCOF1	541 mV at 10 mA cm^{-2}	130	0.5 M H_2SO_4	62
Ru@COF	212 mV at 10 mA cm^{-2}	79	1 M H_2SO_4	63
TpPAM-COF	250 mV at 5 mA cm^{-2}	106	0.5 M H_2SO_4	55
FeS/Fe_3C@N-S-C-800	174 mV at 10 mA cm^{-2}	34	0.5 M H_2SO_4	64
2DP3A	105 mV at 10 mA cm^{-2}	74.1	0.1 M H_2SO_4	65
Ru@COF-1	200 mV at 10 mA cm^{-2}	140	0.5 M H_2SO_4	57
C_6-TRZ-TFP COF	115 mV at 1 mA cm^{-2}	82	-	41
N, P co-doped carbons	260 mV at 10 mA cm^{-2}	175	1.0 M $HClO_4$	66
2.8 wt% Pt-CTF	100 mV at 1 mA cm^{-2}	-	0.1 M $HClO_4$	29
COF@ZIF_{800}	160 mV at 10 mA cm^{-2}	92	1.0 M KOH	47

M H_2SO_4, SB-PORPy COF exhibited superior HER performance to Vulcan and bare glassy carbon with an onset potential of 50 mV and a Tafel slope of 116 mV dec^{-1} (Figure 2c). Furthermore, SB-PORPy COF is a metal-free COF. Authors speculated that the imine nitrogen (-NQ) in COF was protonated under acidic conditions and was an active free docking site for HER. This work demonstrated the potential of metal-free COFs mixed with conductive additive carbon black for electrocatalytic HER. As shown in Figure 2d, Bhaumik et al. reported another metal-free TpPAM COF.[55] As shown in Figure 2e, TpPAM exhibited excellent HER performance at 0.5 M H_2SO_4, with a small Tafel slope of 106 mV dec^{-1} and a low overpotential (250 mV at 10 mA cm^{-2}). The ΔG_{H^*}, calculated to be 0.08 eV, is better than that of most metal-free HER electrocatalysts (Figure 2f, g).

The carbon-carbon double bond is more stable than the current mainstream imine bond in COF.[56] Therefore, stable COFs linked by carbon-carbon double bonds have attractive application prospects in the field of electrochemistry. Meanwhile, covalent triazine frameworks (CTFs) as branches in COFs have the advantages of high porosity, high thermal and chemical stability. In 2022, Chen et al. synthesized Ru@COF-1 by Knoevenagel condensation reaction of 2,4,6-trimethyl-1,3,5-triazine (TMTA) and 1,4-diformylbenzo (DFB), followed by complexation with ruthenium.[57] In acidic media, Ru@COF-1 exhibited excellent HER performance with an overpotential of 200 mV at 10 mA cm^{-2} and a Tafel slope of 140 mV dec^{-1}. Based on DFT calculations, the ΔG_{H^*} of tetracoordinated Ru is 0.09 eV, which is close to 0 eV (Figure 2h).

Combining crystalline porous materials with other compounds such as organic polymers, inorganic active species and so on is a feasible strategy for designing efficient electrocatalysts. Zeng and coworkers constructed a COF and ZIF-67 hybrid with core-shell structure (Figure 2i, j).[47] After pyrolysis, COF@ZIF_{800} displayed a high HER activity with an overpotential of 159 mV at 10 mA cm^{-2} in 1 M KOH electrolyte and a Tafel slope of 92 mV dec^{-1}, which is lower than that of ZIF_{800} (112 mV dec^{-1}). Even though many attempts and efforts have been made, the catalytic performance of existing COF-based catalysts are still far from the benchmark Pt-based catalysts due to the poor conductivity and low stability of COFs under strong acid and base conditions (Table 1). Therefore, future work should focus on the design of COF with strong stability and conductivity.

Hydrogen Oxidation Reaction: HOR is the reverse reaction of HER, so its reaction type and mechanism are similar to HER.[58] HOR is a 2-electron transfer reaction and involves a variety of hydrogen species dependent on the acid-base medium. The HOR reaction is summarized as follows:

Alkaline:

Tafel step: $H_2 \rightarrow 2H_{ads}$ (7)

Heyrovsky step: $H_2 + OH^- \rightarrow H_{ads} + e^- + H_2O$ (8)

Volmer step: $H_{ads} + OH^- \rightarrow e^- + H_2O$ (9)

Acidic:

Tafel step: $H_2 \rightarrow 2H_{ads}$ (10)

Heyrovsky step: $H_2 \rightarrow H_{ads} + H^+ + e^-$ (11)

Volmer step: $H_{ads} \rightarrow e^- + H^+$ (12)

The adsorption energies of H^+ or H_2O/OH^- species in the presence of acids and bases have been proposed as descriptors of HOR reactions and have been used to rationally explain the excellent catalytic performance of platinum.[59] For example, combining Pt with more oxophilic species (Ru or Ni, etc.) will optimize the hydrogen adsorption energy and the hydroxyl adsorption energy, resulting in more optimized HOR activity.[60] Since electrocatalytic HOR is in its nascent stage of development, little work has been done on COF-based applications of HOR. Nakanishi et al. designed single-atom Pt distributing on covalent triazine framework supports, which showed excellent HOR performance as well as oxygen resistance, avoiding Pt corrosion in fuel cells during operation.[29]

n COF-BASED ELECTROCATALYSTS FOR OXYGEN EVOLUTION REACTION AND OXYGEN REDUCTION REACTION

Fuel cells and metal-air batteries are considered ideal technologies for developing efficient and clean energy storage and conversion system.[67] For them, the commonly used fuels or active species hydrogen and oxygen can be obtained by electrocatalytic water splitting. The electricity generated by renewable energy (such as solar and wind energy) can be used to split water to produce hydrogen and oxygen, which are then used as energy carriers to perform HOR and ORR in fuel cells to convert chemical energy into electrical energy. Similarly, OER and ORR can also the half-reactions during charge-discharge in metal-air batteries, which use metals such as sodium, zinc, lithium and alu-

DOI: 10.14102/j.cnki.0254-5861.2022-0162

minum instead of hydrogen as an energy carrier. In this green and sustainable cycle, a steady stream of renewable energy can be converted into chemical energy, and then chemical energy can be converted into electrical energy, which is one of the most ideal energy cycle paths at present. ORR and OER are briefly introduced below.

Oxygen Evolution Reaction: The OER involves four-electron transfer and multiple O-containing intermediates (i.e., OH*, O*, and OOH*), which has slow OER kinetics and large overpotential loss. The four-electron reaction process of oxygen evolution is summarized as follows:[68]

Alkaline:

Total reaction: $4OH^- \rightarrow O_2 + 4e^- + 2H_2O$ (13)

Reaction process: $* + OH^- \rightarrow OH^* + e^-$ (14)

$OH^* + OH^- \rightarrow O^* + H_2O + e^-$ (15)

$O^* + OH^- \rightarrow OOH^* + e^-$ (16)

$OOH^* + OH^- \rightarrow H_2O + O_2 + e^-$ (17)

$O_2^* \rightarrow * + O_2$ (18)

Acidic:

Total reaction: $2H_2O \rightarrow O_2 + 4e^- + 2H^+$ (19)

Reaction process: $* + H_2O \rightarrow OH^* + e^- + H^+$ (20)

$OH^* \rightarrow O^* + H^+ + e^-$ (21)

$O^* + H_2O \rightarrow OOH^* + e^- + H^+$ (22)

$OOH^* \rightarrow 2O^* + H^+ + e^-$ (23)

$OOH^* + OH^- \rightarrow H_2O + O_2 + e^-$ (24)

$O_2^* \rightarrow * + O_2$ (25)

Recently, some COF-based electrocatalytic OER catalysts have been reported. In this section, an overview of the reported typical catalysts and future design directions will be presented.

Similar to HER, OER electrocatalytic performance can be evaluated based on the polarization curve (LSV), overpotential, turnover frequency, Tafel slope, etc. Small Tafel slope values and small overpotential are indications of excellent OER electrocatalysts.[69-72] Recently, efficient OER catalysts are mainly based on noble metal oxides.[73] They can exist stably under acidic condi-

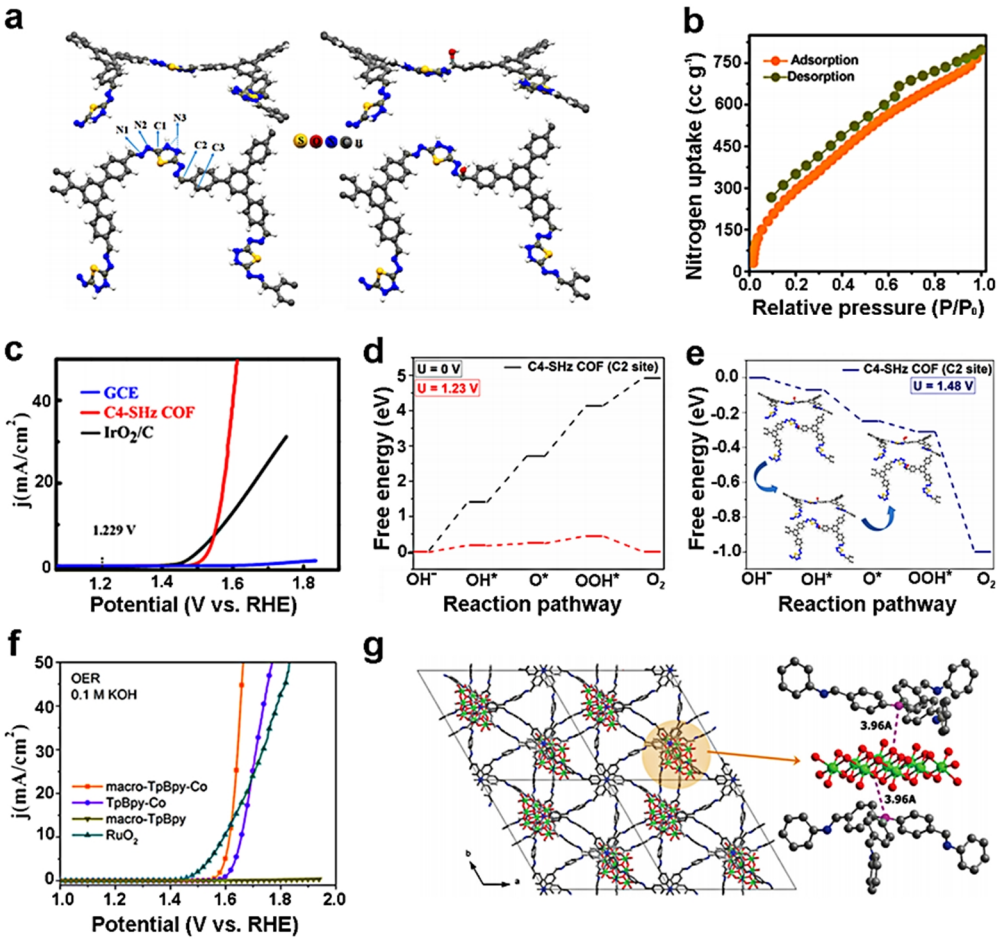

Figure 3. COF-based OER electrocatalyst. (a) Left: DFT calculated optimized structure of the monolayer C4-SHz (different C and N sites are signed), right: most stable structure of the OH* adsorbed C4-SHz surface. (b) N_2 adsorption/desorption isotherms of the C4-SHz COF. (c) OER polarization curve of the C4-SHz COF. (d) Free energy distribution of the OER reaction pathway at U = 0 and 1.23 V for C4-SHz COF's C2 site in alkaline medium. (e) Free energy distribution of the OER reaction pathway at U = 1.48 V.[74] Copyright 2020 American Chemical Society. (f) Polarization curves of macro-TpBpy-Co.[27] Copyright 2019 American Chemical Society. (g) Left: the structure of the model constructed by theoretical calculations of $Ni(OH)_2$ sheets in IISERP-COF2 viewed from the *ab* plane; Right: magnified view along the *bc* plane. The red ball is the sp^3 N center.[79] Copyright 2016 Wiley-VCH.

DOI: 10.14102/j.cnki.0254-5861.2022-0162

tions and have higher catalytic activity than their metallic state. However, large-scale applications are hindered by the rarity and high price of precious metal resources.

COFs have tunable pore structures, which can be tailored to optimize their surface properties, showing great potential as efficient OER electrocatalysts. In 2020, Bhaumik and coworkers reported a metal-free C4-SHz COF (Figure 3a), synthesized by the Schiff base condensation of 1,3,5-tris(4-formylphenyl)benzene and 2,5-dihydrazinyl-1,3,4-thiadiazole through solvothermal method.[74] C4-SHz COF has a high specific surface area of 1224 $m^2 g^{-1}$ (Figure 3b). For OER, C4-SHz COF has a low overpotential of 320 mV at 10 mA cm^{-2} and achieves a low onset potential of 270 mV (Figure 3c), showing potential to replace other metal-free based electrocatalysts. Notably, the interaction between OH^- and N3 or S sites is very weak. Hence, the C2 site is the main active site for OH^- adsorption. Meanwhile, OOH* adsorption was the rate-determining step of the reaction (Figure 3d,e). This work achieved high electrocatalytic OER performance of COFs without hybrid inorganic active materials, demonstrating the application potential of metal-free COF electrocatalysts. Another metal-free work was developed by Zhang et al.[75] According to DFT calculation, the authors constructed a phenazine-linked graphene-like two-dimensional COF (COF-C_4N) via the solvothermal reaction of triphenylhexamine (TPHA) and hexaketocyclohexane (HKH).[75] COF-C_4N showed high OER performance with a Tafel slope of 64 mV dec^{-1}, and an overpotential of 349 mV at 10 mA cm^{-2}. The theoretical modeling calculations showed that the C4 site at the edge was the potential active site for OER. This work provided valuable ideas for the application of metal-free COFs to electrocatalyze OER.

One advantage of COFs is that metals can be incorporated into the framework by metallizing secondary building units, which can enable 2D COFs with enhanced electrocatalytic performance. Co has attracted a lot of attention in the OER field due to its stable redox state.[76] Du et al. combined cobalt porphyrin-based COF with multi-walled carbon nanotubes (abbreviated as (CoP)n-MWCNTs) as a highly efficient OER electrocatalyst[77]. In 1.0 M KOH, as-prepared (CoP)n-MWCNTs showed a low Tafel slope of 60.8 mV dec^{-1} and a low overpotential of 290 mV at 1 mA cm^{-2}. In addition, Kurungot and coworkers reported a covalent organic framework TpBpy containing bipyridine,[78] which was obtained by designing cobalt single atoms into its porous framework via post-processing method. The obtained Co-TpBpy exhibited great OER performance in neutral media, with an overpotential of 400 mV at 1 mA cm^{-2}. Furthermore, Thomas et al. reported a facile strategy to construct well-defined and hierarchical COFs with interconnected macroporous structures (macro-TpBpy-Co).[25] Co^{2+} was coordinated within the hierarchical pore structure, which greatly accelerated ion and mass transport. In 0.1 M KOH, macro-TpBpy-Co displayed a low overpotential of 380 mV at 10 mA cm^{-2} and a low Tafel slope of 54 mV dec^{-1} (Figure 3f), surpassing most reported Co-doped polymer-based OER electrocatalysts. The PS-templated approach used in this work has been extended to gain various macroporous imine-based COFs by tuning the corresponding amine linkers, demonstrating the generality of the method.

Moreover, COFs serve as a support for $Co_xNi_y(OH)_2$ nanoparticles to electrocatalyze OER. The nanoparticles of the resulting hybrid (4Co:12Ni-COF) were well-dispersed (less than 2 nm in size) on COFs, which can achieve high accessibility to catalytic sites.[79] In 1 M KOH solution, the overpotential of 4Co:12Ni-COF at a current density of 10 mA cm^{-2} is only 258 mV, and the Tafel slope is only 38.9 mV dec^{-1}, which is better than that of most reported Ni/Co-based OER catalysts (Table 2). The four-probe test results showed that the support IISERP-COF2-β is non-conductive. The authors established a model to optimize the most stable structure. The nanosheets were sandwiched between two sp^3 nitrogen atoms in adjacent layers (Figure 3g), and the lone pair of electrons in the tetrahedral sp^3 nitrogen center points towards the nanoparticle sheets. This enabled enhanced synergy between the support and nanoparticles, resulting in excellent electrocatalytic OER performance.

Oxygen Reduction Reaction: ORR is a multistep reaction with several intermediates. The process involves the reaction of 4 electrons and 4 protons as well as the cleavage of the double bond in oxygen molecule. The exact mechanism of ORR is still unclear. Generally, O_2 is first adsorbed to the electrode surface, and then it gains electrons and is reduced to H_2O or OH^-. It is a key reaction in the discharge process of fuel cells and metal-air batteries, and determines the working efficiency of these batteries. In general, the ORR process can occur via two distinct pathways: a one-step direct four-electron reduction reaction or a two-step reduction with two electrons in each step. These responses are summarized as follows:

Table 2. List of Some Reported COF-Based Electrocatalysts for OER and Their Experimental Catalytic Activities

OER electrocatalysts	Overpotential (mV)	Tafel slope (mV dec^{-1})	Electrolyte	Ref.
4Co:12Ni-COF	258 mV at 10 mA cm^{-2}	38.9	1.0 M KOH	79
IISERP-COF3/Ni_3N	230 mV at 10 mA cm^{-2}	79	1.0 M KOH	80
C4-SHz COF	320 mV at 10 mA cm^{-2}	39	1.0 M KOH	74
COF-C_4N	349 mV at 10 mA cm^{-2}	64	1.0 M KOH	75
FeS/Fe_3C@N-S-C-800	180 mV at 10 mA cm^{-2}	81	1.0 M KOH	64
Co-TpBpy	400 mV at 1 mA cm^{-2}	-	0.1 M Phosphate buffer	78
Fe_2P/Fe_4N@C-800	410 mV at 10 mA cm^{-2}	177	1.0 M KOH	81
(CoP)n-MWCNTs)	290 mV at 1 mA cm^{-2}	60.8	1.0 M KOH	77
CoCMP	290 mV (j is not mentioned)	87	0.1 M KOH	82
Co_3O_4/NPC	330 mV at 10 mA cm^{-2}	79	1.0 M KOH	83
macro-TpBpy-Co	380 mV at 10 mA cm^{-2}	54	0.1 M KOH	27

DOI: 10.14102/j.cnki.0254-5861.2022-0162

Alkaline:

4-electron reaction process: $O_2 + 4e^- + 2H_2O \rightarrow 4OH^-$ (26)

2+2 electron reaction process:

$O_2 + 2e^- + H_2O \rightarrow HO_2^- + OH^-$ (27)

$HO_2^- + 2e^- + H_2O \rightarrow 3OH^-$ (28)

or disproportionation reaction: $2HO_2^- \rightarrow 2OH^- + O_2$ (29)

Acidic:

4-electron reaction process: $O_2 + 4e^- + 4H^+ \rightarrow 2H_2O$ (30)

2+2 electron reaction process: $O_2 + 2e^- + 2H^+ \rightarrow H_2O_2$ (31)

$H_2O_2 + 2e^- + 2H^+ \rightarrow 2H_2O$ (32)

or disproportionation reaction: $2H_2O_2 \rightarrow 2H_2O + O_2$ (33)

In general, the initial process of the four-electron reaction involves the direct dissociation of O-O bond, which requires more energies than the dissociation of H_2O_2 or HO_2^- (2+2 electron reaction) because the double bond is not broken during the first step of the two-electron process. For further reduction, a higher activation energy is required. The intermediate product H_2O_2 is relatively stable. If the activation energy is not high enough, the reaction may end at any time and become the final product, causing a negative shift in the potential of the electrode. Moreover, the accumulated H_2O_2 can enter the anode and react electrochemically with the metal, resulting in a low utilization of the metal in the metal-air cell. Therefore, the complete reaction of direct four electrons is desired.[84-87]

COFs are regarded as promising ORR electrocatalysts due to their tunable pore structure, large specific surface area, and customizability. Yao and coworkers employed thiophene-sulfur COF (MFTS-COFs) as metal-free ORR electrocatalyst.[24] Two metal-free thiophene-S COFs, JUC-527 and JUC-528, were synthesized and both exhibited superior electrocatalytic ORR performance compared to the thiophene-S COF (PDA-TAPB), demonstrating that the pentacyclic thiophene-S structural unit was the catalytically active center of ORR. Specifically, JUC-528 with irregular particle morphology exhibited the best ORR activity with a half-wave potential of 0.7 V and a Tafel slope of 65.9 mV dec^{-1}, demonstrating its fast kinetics. The number of transferred electrons (n) per O_2 molecule is 3.81 at 0.2 V, which is almost the four-electron transfer behavior of ORR. DFT theoretical modeling calculations (Figure 4a) revealed that JUC-528 possessed a narrower band gap than JUC-527 (Figure 4b). Furthermore, the two adjacent carbon atoms at sites 3 and 5 in pentacyclic thiophene-S showed low overpoentials (Figure 4c), which indicated the key role of thiophene in catalyzing ORR. This work provides a way for subsequent researchers to precisely design electrocatalytic active sites for ORR. Another work on metal-free naphthalene-diimide-based COF (NDI-COF) for ORR is designed by

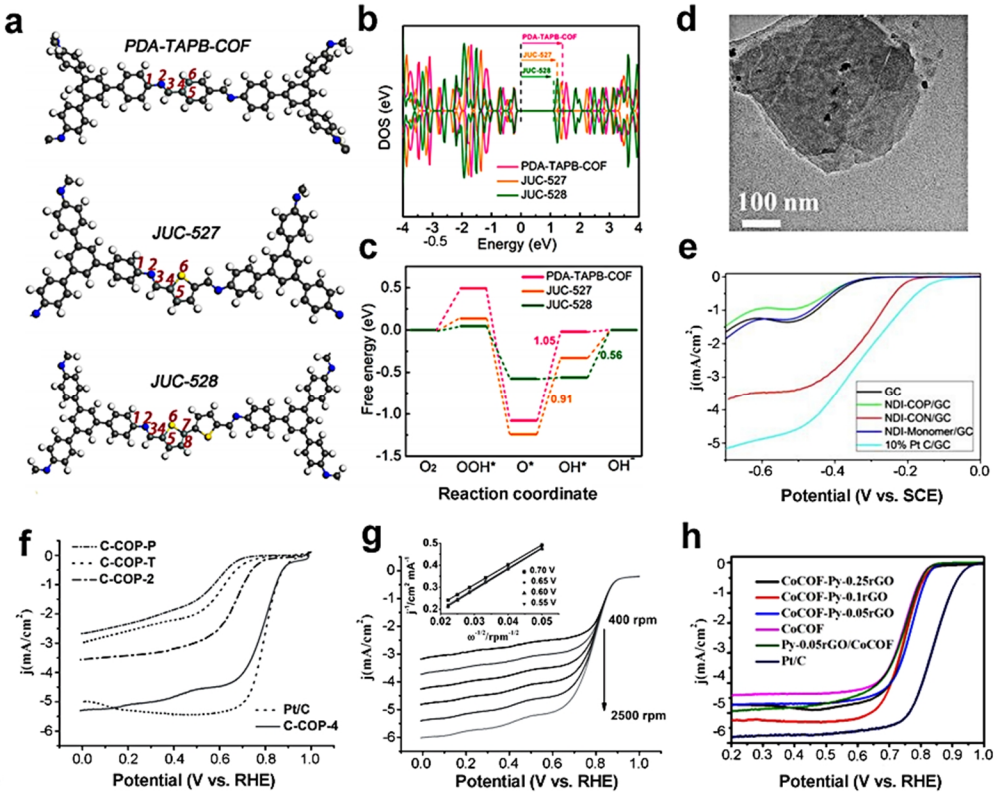

Figure 4. COF-based ORR electrocatalyst. (a) Optimized structures of PDA-TAPB-COF, JUC-527 and JUC-528. S, N, C and H atoms are represented by yellow, blue, gray and white spheres, respectively. (b) DOS and (c) free energy diagrams of the three structures (at site 5).[26] Copyright 2020 American Chemical Society. (d) TEM image of NDI-CONs. (e) ORR polarization curves of NDI-CONs.[88] Copyright 2020 Royal Society of Chemistry. (f) ORR polarization curves of COP graphitic electrodes. (g) Polarization curves of COP graphitic electrodes at different electrode rotation speeds. The inset shows the Koutecky-Levich plot of C-COP-4.[89] Copyright 2014 Wiley-VCH. (h) ORR polarization curves of CoCOF-Py-Rgo.[90] Copyright 2017 Royal Society of Chemistry.

DOI: 10.14102/j.cnki.0254-5861.2022-0162

Table 3. List of Some Reported COF-Based Electrocatalysts for ORR and Their Experimental Catalytic Activities

ORR electrocatalysts	$E_{1/2}$ (V vs. RHE)	Tafel slope (mV dec^{-1})	Electrolyte	Ref.
$COF@ZIF_{800}$	0.85	44	0.1 M KOH	47
N, P co-doped carbons	0.81	70	0.1 M KOH	66
C-COP-4	0.78	-	0.1 M KOH	89
CoCOF-Py-0.05rGO	0.765	61	0.1 M KOH	90
FeS/Fe_3C@N-S-C-800	0.87	90	0.1 M KOH	64
Pt/C	0.84	65	0.1 M KOH	64
$PA@TAPT\text{-}DHTA\text{-}COF_{1000NH3}$	-0.11 (vs. Ag/AgCl)	110	0.1 M KOH	91
COP/rGO	0.72	67.4	0.1 M KOH	44
$Fe_{0.5}Co_{0.5}$Pc-CP NS@G	0.972		0.1 M KOH	92
JUC-528	0.70	65.9	0.1 M KOH	26
$Fe\text{-}C_3N_3\text{-}750\text{-}NH_3$	0.84	75	0.1 M KOH	93

Segura et al.[88] NDI-COFs contained naphthalenediimide (NDI) units, which were considered as promising electron acceptors with electrochemical activity. With a specific surface area of 1138 m^2 g^{-1} and a pore size of 2.5 nm, 2D COF nanosheet material NDI-COF (Figure 4d) exhibited high ORR catalytic activity with an onset potential of -0.25 V, which was better than that of pure GC electrodes (Figure 4e). Also, after 10000 s of operation, the current loss was only ca. 3% with respect to its initial current, demonstrating its excellent stability.

The first metal-free ORR electrocatalyst prepared by COF-derived pyrolysis was reported by Dai et al.[89] Several covalent organic polymers with N-rich structural units were first synthesized, followed by carbonization to obtain graphitic carbon materials with different N-doping levels. The controllably synthesized N-doped porous graphitic carbon material exhibited high ORR electrochemical performance in alkaline media with a half-wave potential of 0.78 V, which was close to that of Pt/C (0.8 V) (Figure 4f, Table 3). In addition, the number of electrons transferred to O_2 molecule was calculated from the Koutecky-Levich (K-L) equation to be 3.90 at 0.55-0.70 V (Figure 4g). This work achieved a breakthrough in the precise control of the position and pore size of N-doped heteroatoms.

The introduction of metals as well as hybrid inorganic active materials into COFs is an important strategy to enhance electrocatalytic performance of ORR. Luo et al. designed a reduced graphene oxide/cobalt porphyrin-based COF (CoCOF-Py-rGO) using pyridine-functionalized reduced graphene oxide (rGO) as the building unit.[90] 4-Styryl pyridine functional groups were present on both sides of rGO as structural nodes connecting the Co-COF, forming a distinctive 3D morphology. CoCOF-Py-rGO achieved high electrocatalytic ORR performance with a half-wave potential of 0.765 V, an onset potential of 0.84 V and a Tafel slope of 61 mV dec^{-1} (Figure 4h, Table 3). It also exhibited higher stability and methanol tolerance in alkaline medium than Pt/C, which was attributed to the synergistic effect of the 3D porous structure of the COF material and the electron transport properties of graphene.

n COF-BASED ELECTROCATALYSTS FOR NITROGEN REDUCTION REACTION

Ammonia is one of the most important chemical raw materials for human production and life, and plays an important role in industrial and agricultural production and energy storage and conversion.[94,95] At present, the industrial ammonia synthesis mainly relies on the energy-intensive Haber-Bosch process, that is, the combined reaction of N_2 and H_2 under the action of a catalyst (iron catalyst) to generate ammonia. This process requires high temperature (> 673 K) under high pressure (> 700 bar), which is very energy-intensive (about 1~2% of the total human energy consumption).[96] Meanwhile, the preparation of synthetic ammonia raw material H_2 also increases the emission of greenhouse gas CO_2 (about 1% of global greenhouse gas emissions). Therefore, the development of sustainable ammonia synthesis technology under normal temperature and pressure is of great strategic significance. The electrochemical nitrogen reduction technology introduces electric energy into the ammonia synthesis reaction, which breaks the high reaction energy barrier of N_2, and realizes the synthesis of ammonia under normal temperature and pressure.

NRR is a six-electron transfer reaction that undergoes three reaction paths and is relatively complex. All three reaction paths undergo the adsorption of N_2 molecules, the breaking of N≡N triple bonds, and the formation of N-H bonds. However, the N≡N triple bonds of N_2 molecules are very strong at room temperature and pressure (bond energy of 941 kJ mol^{-1}), which are difficult to break. Moreover, the similar theoretical potential of NRR and HER leads to the dominance of competing HER, which makes NRR kinetically and thermodynamically difficult to carry out. Hence it is crucial to develop NRR electrocatalysts with high activity and selectivity.

Yan et al. demonstrated that promoting N_2 entry into boron-rich COFs via electrochemical excitation can achieve an efficient NRR catalyst.[86] First, the authors used the metal-free COFs formed by self-condensation of 1,4-benzenediboronic acid (BDBA) as the research model. Figure 5a is the differential charge density map of the electrochemically excited COF (Eex-COF). Yellow represents the lowest unoccupied molecular orbital, and blue-green represents the highest occupied molecular orbitals. Among them, the positive charges are mainly distributed around the boron atom, proving that B in B_3O_3 can serve as the NRR active site. Since kinetic performance is another key point for heterogeneous catalytic systems, the authors also performed MD simulations to investigate whether the above phenomenon was beneficial to the diffusion of nitrogen in the catalyst.

DOI: 10.14102/j.cnki.0254-5861.2022-0162

The results showed that there was a clear distinction between the two models, and N_2 molecules tended to tightly pack around Eex-COF. Subsequently, to confirm the theoretical conclusion, the authors quantitatively investigated the effect of Eex-COF/NC on NRR activity by chronoamperometry using an airtight dual-chamber cell. The LSV curve (Figure 5b) of different states proved that there was a current density difference between N_2 and Ar atmospheres. Figure 5c shows the yields of NH_3 at different constant potentials. Eex-COF/NC achieved an NH_3 yield of 12.53 $\mu g \cdot h^{-1} \cdot mg_{cat}^{-1}$ at -0.2 V and a Faradaic efficiency of 45.43%. In addition, the performance of Eex-COF/NC remained almost unchanged for 10 consecutive cycles of NRR electrolysis, demonstrating its excellent NRR stability.

To overcome the slow kinetics, active metals were introduced into the COFs. Two-dimensional conjugated covalent organic backbones (2D c-COFs) anchored to M-N_x-C centers were reported as NRR electrocatalysts by Feng et al.[28] As-prepared 2D c-COFs (MPc-pz, M=Fe, Co, Ni, Mn, Zn and Cu) were consist of metal phthalocyanine (MPC) and pyrene units, which were bonded by chemically stable pyrazines (Figure 5d). The authors screened different MPc-pz catalysts with M-N_4-C centers, and found FePc-pz showed the best NRR performance with NH_3 yield of 33.6 $\mu g \cdot h^{-1} \cdot mg_{cat}^{-1}$ at -0.1 V and a Faraday efficiency of 31.9%. The rate determining step of NRR on MPc-pz calculated by theoretical modeling was N_2 protonation to form *NNH (Figure 5e). Comparing different atoms, the Fe atom had a localized electronic state at the Fermi energy level making the binding energy of N_2 on Fe-N_4-C stronger, thus the energy barrier was greatly reduced and the NRR kinetics was accelerated.

In 2022, another sophisticated work successfully introduced ordered quasi-phthalocyanine N-coordinated TM (Ti, Cu, or Co) centers into conjugated 2D COFs through a pyrolysis-free synthesis strategy.[98] The transition metal centers (Ti, Cu, or Co) were anchored to the corresponding COF frameworks in the form of coordination structure (Figure 5f). There was a large current density gap in the LSV curves of Ti-COF (Figure 5g) under N_2 and Ar, which proved that the NRR had already happened. Then, Ti-COF had a high NH_3 yield of 26.89 $\mu g \cdot h^{-1} \cdot mg_{cat}^{-1}$ and a Faradaic efficiency of 34.62%, which was superior to that of Cu-COF and Co-COF. DFT calculations of NRR transition states confirmed that NRR tends to undergo alternate paths rather than the distal paths on Ti-COF (Figure 5h). Furthermore, the comparison of the partial density of states (PDOS) of Ti-COF before and after nitrogen activation indicated that Ti-COF could adsorb and activate N_2 molecules, and efficiently inhibit HER side reactions, thereby improving NRR catalytic activity. This work provides a

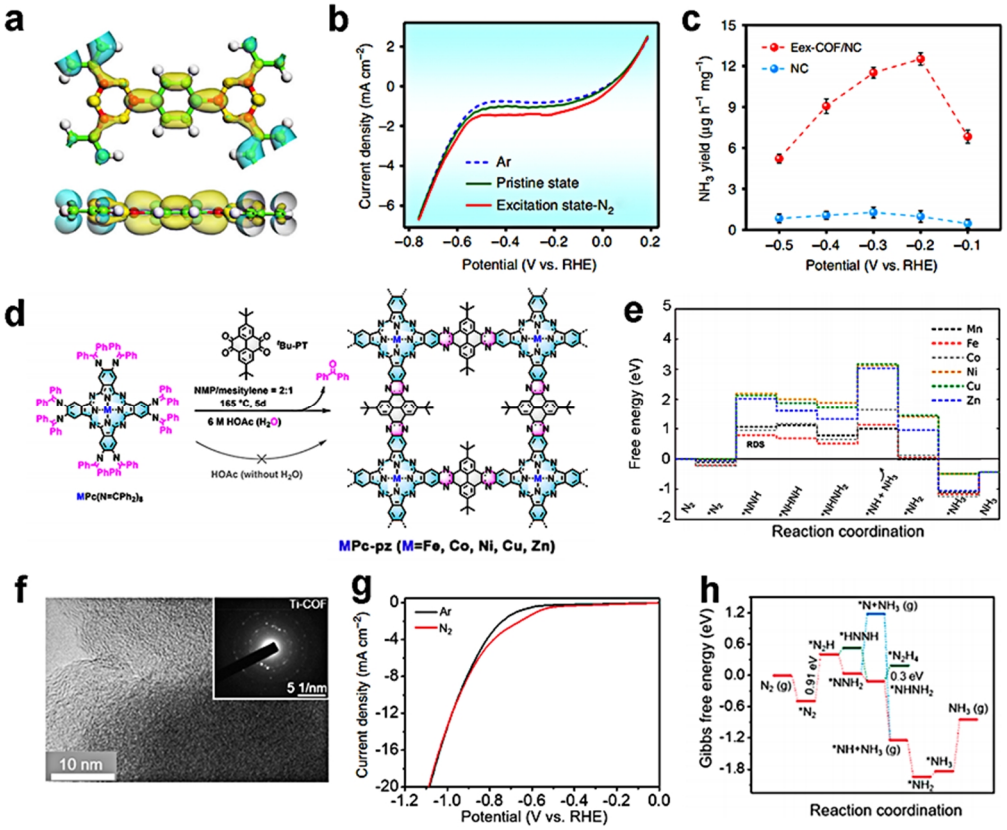

Figure 5. COF-based NRR electrocatalyst. (a) The calculated charge distribution of COF. (b) Polarization curve of different states through excitation. (c) NH_3 yield of Eex-COF.[97] Copyright 2019 Nature Publishing Group. (d) Schematic synthetic process of MPc-pz. (e) Free energy distribution of NRR along alternate paths on MPc-pz.[28] Copyright 2021 American Chemical Society. (f) HRTEM and SAED (inset) images of Ti-COF. (g) Polarization curve of Ti-COF in Ar- and N_2-saturated 0.05 M HCl electrolyte. (h) DFT calculated reaction energy diagram of NRR for Ti-COF.[98] Copyright 2022 American Chemical Society.

DOI: 10.14102/j.cnki.0254-5861.2022-0162

valuable idea for the development of 2D COFs electrocatalytic materials with rich coordination transition metal centers.

n COF-BASED ELECTROCATALYSTS FOR CARBON DIOXIDE REDUCTION REACTION

The continuous consumption of non-renewable fossil fuels not only causes the energy crisis, but also leads to a series of climate problems such as global warming caused by the continuous increase in the concentration of carbon dioxide (CO_2) in the atmosphere, which breaks the natural carbon cycle process.[99] Therefore, the effective utilization and conversion of CO_2 have received extensive attention. The electrochemical reduction of CO_2 can be driven by renewable energy to convert CO_2 into chemicals, which is considered to be one of the promising ways for CO_2 conversion and utilization. Meanwhile, the formation of target products can be selectively controlled by changing the electrolysis conditions. However, given the stable linear structure of CO_2 molecules, it is urgent to design and synthesize cheap, efficient and stable electrocatalysts to catalyze CO_2RR. COFs have been used as electrocatalysts in the field of CO_2RR due to their large specific surface area and easy functionalization.

The electrochemical CO_2RR is a multi-step reaction process involving 2, 4, 6, 8, 10 and other multiple electron transfer pathways. It generally includes the following key steps: 1) chemisorption of CO_2 molecules on the surface of solid-state catalysts; 2) transfer of electrons and protons to tear C-O bonds and form C-H bonds, etc.; 3) product structure rearrangement and desorption from the catalyst surface into the electrolyte. In 2015, Yaghi et al.[39] synthesized two COFs (COF-366-Co and COF-367-Co) by the reactions of 5,10,15,20-tetrakis(4-aminophenyl) porphinato cobalt and 1,4-benzenedicarbaldehyde (BDA), biphenyl-4,4'-dicarbaldehyde (BPDA), respectively (Figure 6a, b). The authors deposited COF materials on porous conductive carbon fabrics. The catalyst exhibited the best catalytic performance at a potential of -0.67 V (Figure 6c). COF-366-Co promoted the release of carbon monoxide at an initial current density of 5 mA mg^{-1}. The Faradaic efficiency of the catalyst ($\approx$80 mA mg^{-1}_{Co}) is 90%. This work shows the kinetics of the catalytic process can be significantly improved by designing a special structure to make the catalytic active site contact with the reactants efficiently.

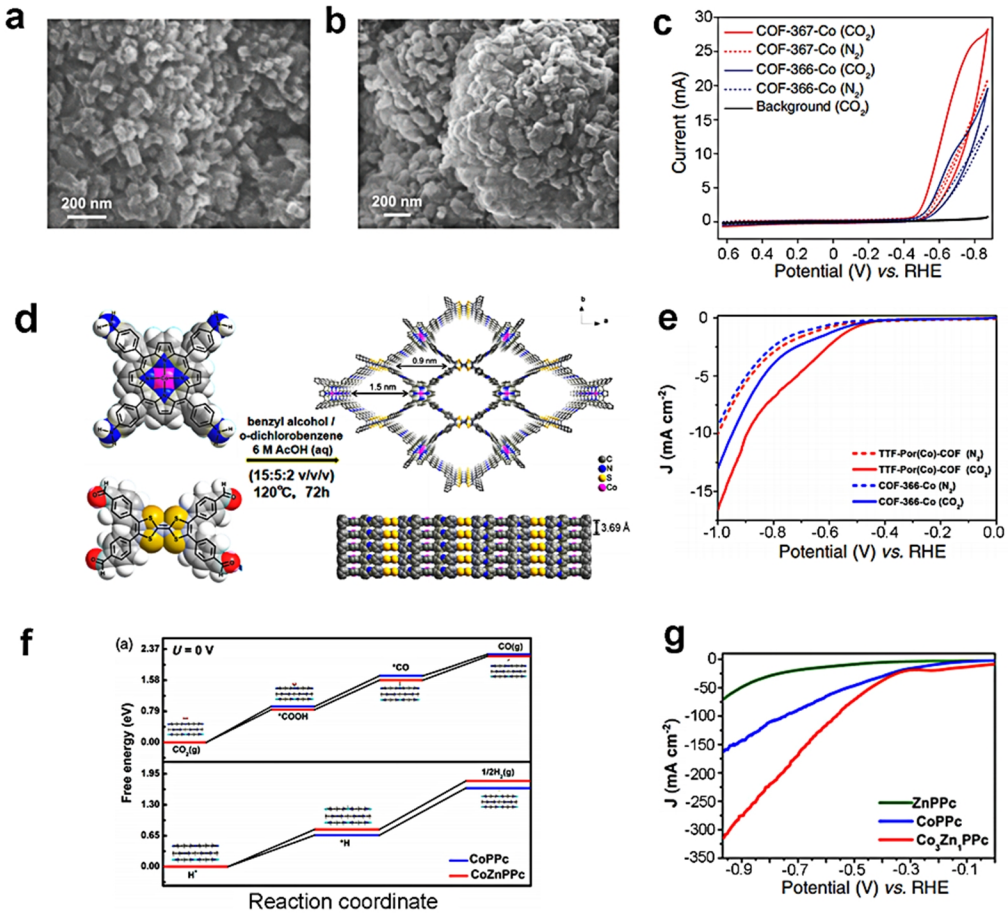

Figure 6. COF-based CO_2RR electrocatalyst. (a) SEM image of COF-366-Co. (b) SEM image of COF-367-Co. (c) CVs of COF-366-Co and COF-367-Co in CO_2-saturated medium (blue and red solid lines, respectively) or N_2-saturated medium (blue and red dotted lines, respectively).[39] Copyright 2015 The American Association for the Advancement of Science. (d) Synthetic schematic illustration of TTF-Por(Co)-COF with views along the c axis (upper right) and side views (lower right). (e) LSV curves of TTF-Por(Co)-COF and COF-366-Co in the N_2-saturated and CO_2-saturated 0.5 M $KHCO_3$ electrolyte.[100] Copyright 2020 American Chemical Society. (f) Free energy diagram for CO_2RR (up) and HER (down) at pH 14 on the Co site in CoPPc and CoZnPPc, respectively. (g) LSV curves of CoPPc, ZnPPc, and Co_3Zn_1PPc in 1 M KOH electrolyte under CO_2.[5] Copyright 2022 Chinese Chemical Society.

DOI: 10.14102/j.cnki.0254-5861.2022-0162

As shown in Figure 6d, Cao and coworkers incorporated tetrathiafulvalene (TTF) into the framework of two-dimensional porphyrin COFs.[100] TTF-Por(Co)-COF was endowed with better electron transfer ability than COF-366-Co without TTF, which could improve the catalytic activity (Figure 6e). For CO_2RR, Faradaic efficiency of TTF-Por(Co)-COF reached 95%. Meanwhile, it has good stability at a constant voltage of -0.7 V. Compared with COF-366-Co, TTF-Por(Co)-COF required a lower energy to complete the rate-limiting step of CO_2 reduction to *COOH, assisted by DFT calculations. In addition, Cao et al.[5] optimized the energy and bonding strength of the reaction intermediates by introducing electron-rich Zn into CoPPc (Figure 6f). Co in the electron-rich region was the catalytic active sites and showed excellent CO_2RR catalytic performance with 90% Faraday efficiency (Figure 6g). This work opens a universal avenue for applying COF materials as the CO_2RR electrocatalysts.

n CONCLUSIONS AND PERSPECTIVES

Since the invention of COFs by Yaghi et al. in 2005, COFs with different structures have been designed and synthesized for different application fields. COFs are promising electrocatalysts with customizable structures, tunable pore structures, abundant active sites, and functional groups. This review summarizes the design strategies of COF-based electrocatalysts, including (1) using COFs as supports, (2) introduction of active metals into COFs, (3) exfoliating COFs to two-dimensional conductive nanosheet, (4) compositing COFs with inorganic active species, and (5) pyrolysis of COFs to obtain carbon-based materials, etc. Specific structures are precisely prepared at the molecular/atomic level by the above strategies to enhance the content of active sites and improve intrinsic activity of each active site. Furthermore, COF-based electrocatalysts have made great progress in specific electrocatalytic reactions recently, including hydrogen catalysis (HER and HOR), oxygen catalysis (OER and ORR), NRR and CO_2RR. This review summarizes the key parameters of various electrocatalytic reactions in a tabular form to clearly compare the electrocatalysts. Although staged progress has been made in the development of COF-based electrocatalysts, there are still several issues worthy of further exploration.

First, whether it is the relatively mature fields of HER, OER and ORR or the fields of HOR, NRR and CO_2RR in their infancy, there are problems of slow reaction kinetics. Meanwhile, the origin of slow kinetics has not been fully determined, and its fundamental basis remains to be explained. From an experimental point of view, it is strongly recommended to analyze the COF single crystal structure by single crystal means for a deep understanding of the material. In situ spectroscopy and microscopy techniques, such as Raman spectroscopy, TEM, and in situ XPS, can also be used to monitor the occurrence and subtle changes of the catalytic reaction process. This can observe the interaction and banding strength of each catalytic reaction intermediate in real time, which will help us understand the basic properties of electrocatalytic reactions. Furthermore, DFT calculations are invaluable tools for revealing the realistic catalytic processes and for identifying true active sites. The calculated results can provide important information for understanding the effects of various reaction intermediates, adsorption free energy, descriptors, etc. on the reaction rate. Though the current theoretical calculations are concerned, it is still a huge challenge to reasonably correlate the active sites of the theoretical model with the experimentally obtained phenomena under real catalytic conditions, and further research and exploration are needed.

Second, the active sites and microstructures of COF-based electrocatalysts should be more precisely controlled. The precise tuning of building blocks to fully exploit the intrinsic advantages of COFs largely determines the catalytic activity. Moreover, the synergistic effect between COFs and the load, carrier or composite species also needs to be further considered, which is one of the critical factors affecting the catalytic performance. In addition, the low intrinsic conductivity of COFs is a key limitation as an efficient electrocatalyst. At present, some researchers have successfully improved their conductivity by constructing two-dimensional conductive COFs or pyrolyzing COFs to obtain carbon materials. Apart from that, heteroatomic hybridization is also a promising method to improve the electrical conductivity of COFs. The COFs with improved electrical conductivity can quickly supply the required electrons for electrocatalytic reactions, thereby enhancing the catalytic activity.

Third, the stability of electrocatalysts is crucial for various specific electrocatalytic reactions, especially under strong acid and base conditions. Almost none of the reported COF electrocatalysts are stable for tens of hours, far from meeting the practical application requirements for stable maintenance. In order to improve the electrocatalytic stability of COFs, the factors that determine the stability, including the composition, microstructure, and hydrophilicity and hydrophobicity of building blocks, should be accurately judged and controlled. Meanwhile, various characterization methods can be used to monitor the active degradation process or framework collapse process of COFs, which will reveal the mechanism and provide guidance for the design of highly stable electrocatalysts.

n ACKNOWLEDGEMENTS

This work was supported by the National Natural Science Foundation of China (52101268) and Tianjin Natural Science Foundation (19JCQNJC05000).

n AUTHOR INFORMATION

Corresponding authors. Emails: hxxyshm@tjnu.edun.cn (Hongming Sun) and hxxylcp@tjnu.edu.cn (Cheng-Peng Li)

n COMPETING INTERESTS

The authors declare no competing interests.

n ADDITIONAL INFORMATION

Full paper can be accessed via
http://manu30.magtech.com.cn/jghx/EN/10.14102/j.cnki.0254-5861.2022-0162
For submission: https://www.editorialmanager.com/cjschem

n REFERENCES

(1) Liang, J.; Wu, Q.; Huang, Y. B.; Cao, R. Reticular frameworks and

their derived materials for CO_2 conversion by thermo-catalysis. *Energy-Chem.* **2021**, 3, 100046.

(2) Guo, H.; Si, D. H.; Zhu, H. J.; Li, Q. X.; Huang, Y. B.; Cao, R. Ni single-atom sites supported on carbon aerogel for highly efficient electroreduction of carbon dioxide with industrial current densities. *eScience* **2022**, 2, 295-303.

(3) Su, H.; Soldatov, M. A.; Roldugin, V.; Liu, Q. Platinum single-atom catalyst with self-adjustable valence state for large-current-density acidic water oxidation. *eScience* **2022**, 2, 102-109.

(4) Seh, Z. W.; Kibsgaard, J.; Dickens, C. F.; Chorkendorff, I.; Nørskov, J. K.; Jaramillo, T. F. Combining theory and experiment in electrocatalysis: insights into materials design. *Science* **2017**, 355, 6321.

(5) Li, N.; Si, D. H.; Wu, Q. J.; Wu, Q.; Huang, Y. B.; Cao, R. Boosting electrocatalytic CO_2 reduction with conjugated bimetallic Co/Zn polyphthalocyanine frameworks. *CCS Chem.* **2022**, DOI: 10.31635/ccschem.022.202201943.

(6) McCrory, C. C.; Jung, S.; Ferrer, I. M.; Chatman, S. M.; Peters, J. C.; Jaramillo, T. F. Benchmarking hydrogen evolving reaction and oxygen evolving reaction electrocatalysts for solar water splitting devices. *J. Am. Chem. Soc.* **2015**, 137, 4347-4357.

(7) Liu, M.; Wei, C.; Zhuzhang, H.; Zhou, J.; Pan, Z.; Lin, W.; Yu, Z.; Zhang, G.; Wang, X. Fully condensed poly(triazine imide) crystals: extended pi-conjugation and structural defects for overall water splitting. *Angew. Chem. Int. Ed.* **2022**, 61, e202113389.

(8) Zhai, P.; Xia, M.; Wu, Y.; Zhang, G.; Gao, J.; Zhang, B.; Cao, S.; Zhang, Y.; Li, Z.; Fan, Z.; Wang, C.; Zhang, X.; Miller, J. T.; Sun, L.; Hou, J. Engineering single-atomic ruthenium catalytic sites on defective nickel-iron layered double hydroxide for overall water splitting. *Nat. Commun.* **2021**, 12, 4587.

(9) Oh, N. K.; Seo, J.; Lee, S.; Kim, H. J.; Kim, U.; Lee, J.; Han, Y. K.; Park, H. Highly efficient and robust noble-metal free bifunctional water electrolysis catalyst achieved via complementary charge transfer. *Nat. Commun.* **2021**, 12, 4606.

(10) Dai, L.; Chen, Z. N.; Li, L.; Yin, P.; Liu, Z.; Zhang, H. Ultrathin Ni(0)-embedded $Ni(OH)_2$ heterostructured nanosheets with enhanced electrochemical overall water splitting. *Adv. Mater.* **2020**, 32, 1906915.

(11) Yu, Y.; Zhou, J.; Sun, Z. Novel 2D transition-metal carbides: ultrahigh performance electrocatalysts for overall water splitting and oxygen reduction. *Adv. Funct. Mater.* **2020**, 30, 2000570.

(12) Kim, S.; Koratkar, N.; Karabacak, T.; Lu, T.-M. Water electrolysis activated by Ru nanorod array electrodes. *Appl. Phys. Lett.* **2006**, 88, 263106.

(13) Wang, T.; Cao, X; Jiao, L. Ni_2P/NiMoP heterostructure as a bifunctional electrocatalyst for energy-saving hydrogen production. *eScience.* **2021**, 1, 69-74.

(14) Zhang, Q.; Wang, Y.; Wang, Y.; Yang, S.; Wu, X.; Lv, B.; Wang, N.; Gao, Y.; Xu, X.; Lei, H.; Cao, R. Electropolymerization of cobalt porphyrins and corroles for the oxygen evolution reaction. *Chin. Chem. Lett.* **2021**, 32, 3807-3810.

(15) Wang, W.; Wang, Z.; Hu, Y.; Liu, Y.; Chen, S. A potential-driven switch of activity promotion mode for the oxygen evolution reaction at Co_3O_4/NiO_xH_y interface. *eScience.* **2022**, Doi: doi.org/10.1016/j.esci.2022.04.004.

(16) Guo, X.; Wan, X.; Liu, Q.; Liu, Y.; Li, W.; Shui, J. Phosphated IrMo bimetallic cluster for efficient hydrogen evolution reaction. *eScience.* **2022**, doi.org/10.1016/j.esci.2022.04.002.

(17) Long, X.; Meng, J.; Gu, J.; Ling, L.; Li, Q.; Liu, N.; Wang, K.; Li, Z. Interfacial engineering of NiFeP/NiFe-LDH heterojunction for efficient overall water splitting. *Chin. J. Struct. Chem.* **2022**, 41, 2204046-2204053.

(18) He, C.; Liang, J.; Zou, Y. H.; Yi, J. D.; Huang, Y. B.; Cao, R. Metal-organic frameworks bonded with metal N-heterocyclic carbenes for efficient catalysis. *Natl. Sci. Rev.* **2022**, 9, nwab157.

(19) Niu, J.; Shao, R.; Liu, M.; Zan, Y.; Dou, M.; Liu, J.; Zhang, Z.; Huang, Y.; Wang, F. Porous carbons derived from collagen-enriched biomass: tailored design, synthesis, and application in electrochemical energy storage and conversion. *Adv. Funct. Mater.* **2019**, 29, 1905095.

(20) Geng, K.; He, T.; Liu, R.; Dalapati, S.; Tan, K. T.; Li, Z.; Tao, S.; Gong, Y.; Jiang, Q.; Jiang, D. Covalent organic frameworks: design, synthesis, and functions. *Chem. Rev.* **2020**, 120, 8814-8933.

(21) Xu, S.; Zhang, Q. Recent progress in covalent organic frameworks as light-emitting materials. *Mater. Today Energy* **2021**, 20, 100635.

(22) Cote, A. P.; Benin, A. I.; Ockwig, N. W.; O'Keeffe, M.; Matzger, A. J.; Yaghi, O. M. Porous, crystalline, covalent organic frameworks. *Science* **2005**, 310, 1166-1170.

(23) Wang, P. L.; Ding, S. Y.; Zhang, Z. C.; Wang, Z. P.; Wang, W. Constructing robust covalent organic frameworks via multicomponent reactions. *J. Am. Chem. Soc.* **2019**, 141, 18004-18008.

(24) Huang, X.; Sun, C.; Feng, X. Crystallinity and stability of covalent organic frameworks. *Sci. China Chem.* **2020**, 63, 1367-1390.

(25) Tan, K. T.; Tao, S.; Huang, N.; Jiang, D. Water cluster in hydrophobic crystalline porous covalent organic frameworks. *Nat. Commun.* **2021**, 12, 6747.

(26) Li, D.; Li, C.; Zhang, L.; Li, H.; Zhu, L.; Yang, D.; Fang, Q.; Qiu, S.; Yao, X. Metal-free thiophene-sulfur covalent organic frameworks: precise and controllable synthesis of catalytic active sites for oxygen reduction. *J. Am. Chem. Soc.* **2020**, 142, 8104-8108.

(27) Zhao, X.; Pachfule, P.; Li, S.; Langenhahn, T.; Ye, M.; Schlesiger, C.; Praetz, S.; Schmidt, J.; Thomas, A. Macro/microporous covalent organic frameworks for efficient electrocatalysis. *J. Am. Chem. Soc.* **2019**, 141, 6623-6630.

(28) Zhong, H.; Wang, M.; Ghorbani-Asl, M.; Zhang, J.; Ly, K. H.; Liao, Z.; Chen, G.; Wei, Y.; Biswal, B. P.; Zschech, E.; Weidinger, I. M.; Krasheninnikov, A. V.; Dong, R.; Feng, X. Boosting the electrocatalytic conversion of nitrogen to ammonia on metal-phthalocyanine-based two-dimensional conjugated covalent organic frameworks. *J. Am. Chem. Soc.* **2021**, 143, 19992-20000.

(29) Kamai, R.; Kamiya, K.; Hashimoto, K.; Nakanishi, S. Oxygen-tolerant electrodes with platinum-loaded covalent triazine frameworks for the hydrogen oxidation reaction. *Angew. Chem. Int. Ed.* **2016**, 55, 13184-13188.

(30) Bhunia, S.; Das, S. K.; Jana, R.; Peter, S. C.; Bhattacharya, S.; Addicoat, M.; Bhaumik, A.; Pradhan, A. Electrochemical stimuli-driven facile metal-free hydrogen evolution from pyrene-porphyrin-based crystalline covalent organic framework. *ACS Appl. Mater. Interfaces* **2017**, 9, 23843-23851.

(31) Lin, C. Y.; Zhang, D. T.; Zhao, Z. H.; Xia, Z. H. Covalent organic framework electrocatalysts for clean energy conversion. *Adv. Mater.* **2018**, 30, 1801726.

(32) Bleier, G. C.; Watt, J.; Simocko, C. K.; Lavin, J. M.; Huber, D. L. Reversible magnetic agglomeration: a mechanism for thermodynamic control over nanoparticle size. *Angew. Chem. Int. Ed.* **2018**, 57, 7678-7681.

DOI: 10.14102/j.cnki.0254-5861.2022-0162

(33) Lee, H.; Nedrygailov, II; Lee, C.; Somorjai, G. A.; Park, J. Y. Chemical-reaction-induced hot electron flows on platinum colloid nanoparticles under hydrogen oxidation: impact of nanoparticle size. *Angew. Chem. Int. Ed.* **2015**, 54, 2340-2344.

(34) Fox, E. K.; El Haddassi, F.; Hierrezuelo, J.; Ninjbadgar, T.; Stolarczyk, J. K.; Merlin, J.; Brougham, D. F. Size-controlled nanoparticle clusters of narrow size-polydispersity formed using multiple particle types through competitive stabilizer desorption to a liquid-liquid Interface. *Small* **2018**, 14, 1802278.

(35) Yang, H.; Liu, Y.; Liu, X.; Wang, X.; Tian, H.; Waterhouse, G. I. N.; Kruger, P. E.; Telfer, S. G.; Ma, S. Large-scale synthesis of N-doped carbon capsules supporting atomically dispersed iron for efficient oxygen reduction reaction electrocatalysis. *eScience* **2022**, 2, 227-234.

(36) Cao, Y.; Peng, W.; Li, Y.; Zhang, F.; Zhu, Y.; Fan, X. Atomically dispersed metal sites in COF-based nanomaterials for electrochemical energy conversion. *Green Energy & Environment.* **2021**. doi.org/10.1016/j.gee.2021.11.005.

(37) Gunasekar, G. H.; Park, K.; Ganesan, V.; Lee, K.; Kim, N.-K.; Jung, K.-D.; Yoon, S. A covalent triazine framework, functionalized with Ir/N-heterocyclic carbene sites, for the efficient hydrogenation of CO_2 to formate. *Chem. Mater.* **201**7, 29, 6740-6748.

(38) Hosokawa, T.; Tsuji, M.; Tsuchida, K.; Iwase, K.; Harada, T.; Nakanishi, S.; Kamiya, K. Metal-doped bipyridine linked covalent organic framework films as a platform for photoelectrocatalysts. *J. Mater. Chem. A* **2021**, 9, 11073-11080.

(39) Lin, S.; Diercks, C. S.; Zhang, Y. B.; Kornienko, N.; Nichols, E. M.; Zhao, Y.; Paris, A. R.; Kim, D.; Yang, P.; Yaghi, O. M.; Chang, C. J. Covalent organic frameworks comprising cobalt porphyrins for catalytic CO_2 reduction in water. *Science* **2015**, 349, 1208-1213.

(40) Yusran, Y.; Li, H.; Guan, X.; Li, D.; Tang, L.; Xue, M.; Zhuang, Z.; Yan, Y.; Valtchev, V.; Qiu, S.; Fang, Q. Exfoliated mesoporous 2D covalent organic frameworks for high-rate electrochemical double-layer capacitors. *Adv. Mater.* **2020**, 32, 1907289.

(41) Ruidas, S.; Mohanty, B.; Bhanja, P.; Erakulan, E. S.; Thapa, R.; Das, P.; Chowdhury, A.; Mandal, S. K.; Jena, B. K.; Bhaumik, A. Metal-free triazine-based 2D covalent organic framework for efficient H_2 evolution by electrochemical water splitting. *Chemsuschem.* **2021**, 14, 5057-5064.

(42) Jin, E.; Fu, S.; Hanayama, H.; Addicoat, M. A.; Wei, W.; Chen, Q.; Graf, R.; Landfester, K.; Bonn, M.; Zhang, K. A. I.; Wang, H. I.; Mullen, K.; Narita, A. A nanographene-based two-dimensional covalent organic framework as a stable and efficient photocatalyst. *Angew. Chem. Int. Ed.* **2022**, 61, e202114059.

(43) Xu, F.; Chen, X.; Tang, Z.; Wu, D.; Fu, R.; Jiang, D. Redox-active conjugated microporous polymers: a new organic platform for highly efficient energy storage. *Chem. Commun.* **2014**, 50, 4788-4790.

(44) Guo, J.; Lin, C. Y.; Xia, Z.; Xiang, Z. A pyrolysis-free covalent organic polymer for oxygen reduction. *Angew. Chem. Int. Ed.* **2018**, 57, 12567-12572.

(45) Hijazi, I.; Bourgeteau, T.; Cornut, R.; Morozan, A.; Filoramo, A.; Leroy, J.; Derycke, V.; Jousselme, B.; Campidelli, S. Carbon nanotube-templated synthesis of covalent porphyrin network for oxygen reduction reaction. *J. Am. Chem. Soc.* **2014**, 136, 6348-6354.

(46) Li, C.; Xi, Z.; Guo, D.; Chen, X.; Yin, L. Chemical immobilization effect on lithium polysulfides for lithium-sulfur batteries. *Small* **2018**, 14, 1701986.

(47) Liu, M.; Xu, Q.; Miao, Q.; Yang, S.; Wu, P.; Liu, G.; He, J.; Yu, C.; Zeng, G. Atomic Co-N_4 and Co nanoparticles confined in COF@ZIF-67 derived core-shell carbon frameworks: bifunctional non-precious metal catalysts toward the ORR and HER. *J. Mater. Chem. A* **2022**, 10, 228-233.

(48) Guo, C.; Duan, F.; Zhang, S.; He, L.; Wang, M.; Chen, J.; Zhang, J.; Jia, Q.; Zhang, Z.; Du, M. Heterostructured hybrids of metal-organic frameworks (MOFs) and covalent-organic frameworks (COFs). *J. Mater. Chem. A* **2022**, 10, 475-507.

(49) Zhao, W.; Jin, B.; Wang, L.; Ding, C.; Jiang, M.; Chen, T.; Bi, S.; Liu, S.; Zhao, Q. Ultrathin Ti_3C_2 nanowires derived from multi-layered bulks for high-performance hydrogen evolution reaction. *Chin. Chem. Lett.* **2022**, 33, 557-561.

(50) Li, D.; Park, E. J.; Zhu, W.; Shi, Q.; Zhou, Y.; Tian, H.; Lin, Y.; Serov, A.; Zulevi, B.; Baca, E. D.; Fujimoto, C.; Chung, H. T.; Kim, Y. S. Highly quaternized polystyrene ionomers for high performance anion exchange membrane water electrolysers. *Nat. Energy* **2020**, 5, 378-385.

(51) Wang, L.; Bellini, M.; Miller, H. A.; Varcoe, J. R. A high conductivity ultrathin anion-exchange membrane with 500+ h alkali stability for use in alkaline membrane fuel cells that can achieve 2 W cm^{-2} at 80 °C. *J. Mater. Chem. A* **2018**, 6, 15404-15412.

(52) Yang, F.; Han, P.; Yao, N.; Cheng, G.; Chen, S.; Luo, W. Inter-regulated d-band centers of the Ni_3B/Ni heterostructure for boosting hydrogen electrooxidation in alkaline media. *Chem. Sci.* **2020**, 11, 12118-12123.

(53) Sun, H.; Tian, C.; Fan, G.; Qi, J.; Liu, Z.; Yan, Z.; Cheng, F.; Chen, J.; Li, C. P.; Du, M. Boosting activity on Co_4N porous nanosheet by coupling CeO_2 for efficient electrochemical overall water splitting at high current densities. *Adv. Funct. Mater.* **2020**, 30, 1910596.

(54) Zheng, Y.; Jiao, Y.; Jaroniec, M.; Qiao, S. Z. Advancing the electrochemistry of the hydrogen-evolution reaction through combining experiment and theory. *Angew. Chem. Int. Ed.* **2015**, 54, 52-65.

(55) Patra, B. C.; Khilari, S.; Manna, R. N.; Mondal, S.; Pradhan, D.; Pradhan, A.; Bhaumik, A. A metal-free covalent organic polymer for electrocatalytic hydrogen evolution. *ACS Catal.* **2017**, 7, 6120-6127.

(56) Zhuang, X.; Zhao, W.; Zhang, F.; Cao, Y.; Liu, F.; Bi, S.; Feng, X. A two-dimensional conjugated polymer framework with fully sp^2-bonded carbon skeleton. *Polym. Chem.* **2016**, 7, 4176-4181.

(57) Zhao, Y. X.; Liang, Y.; Wu, D. X.; Tian, H.; Xia, T.; Wang, W. X.; Xie, W. Y.; Hu, X. M.; Tian, X. L.; Chen, Q. Ruthenium complex of sp^2 carbon-conjugated covalent organic frameworks as an efficient electrocatalyst for hydrogen evolution. *Small* **2022**, 18, 2107750.

(58) Durst, J.; Siebel, A.; Simon, C.; Hasche, F.; Herranz, J.; Gasteiger, H. A. New insights into the electrochemical hydrogen oxidation and evolution reaction mechanism. *Energy Environ. Sci.* **2014**, 7, 2255-2260.

(59) Strmcnik, D.; Uchimura, M.; Wang, C.; Subbaraman, R.; Danilovic, N.; van der Vliet, D.; Paulikas, A. P.; Stamenkovic, V. R.; Markovic, N. M. Improving the hydrogen oxidation reaction rate by promotion of hydroxyl adsorption. *Nat. Chem.* **2013**, 5, 300-306.

(60) Zhu, S.; Qin, X.; Xiao, F.; Yang, S.; Xu, Y.; Tan, Z.; Li, J.; Yan, J.; Chen, Q.; Chen, M.; Shao, M. The role of ruthenium in improving the kinetics of hydrogen oxidation and evolution reactions of platinum. *Nat. Catal.* **2021**, 4, 711-718.

(61) Jia, H.; Yao, Y.; Gao, Y.; Lu, D.; Du, P. Pyrolyzed cobalt porphyrin-based conjugated mesoporous polymers as bifunctional catalysts for hydrogen production and oxygen evolution in water. *Chem. Commun.*

DOI: 10.14102/j.cnki.0254-5861.2022-0162

2016, 52, 13483-13486.
(62) Zhou, D.; Tan, X.; Wu, H.; Tian, L.; Li, M. Synthesis of C-C bonded two-dimensional conjugated covalent organic framework films by Suzuki polymerization on a liquid-liquid interface. *Angew. Chem. Int. Ed.* **2019**, 58, 1376-1381.
(63) Maiti, S.; Chowdhury, A. R.; Das, A. K. Electrochemically facile hydrogen evolution using ruthenium encapsulated two dimensional covalent organic framework (2D COF). *ChemNanoMat.* **2019**, 6, 99-106.
(64) Kong, F.; Fan, X.; Kong, A.; Zhou, Z.; Zhang, X.; Shan, Y. Covalent phenanthroline framework derived FeS@Fe_3C composite nanoparticles embedding in N-S-Co doped carbons as highly efficient trifunctional electrocatalysts. *Adv. Funct. Mater.* **2018**, 28, 1803973.
(65) Ranjeesh, K. C.; Illathvalappil, R.; Wakchaure, V. C.; Goudappagouda; Kurungot, S.; Babu, S. S. Metalloporphyrin two-dimensional polymers via metal-catalyst-free C-C bond formation for efficient catalytic hydrogen evolution. *ACS Appl. Energy Mater.* **2018**, 1, 6442-6450.
(66) Yang, C.; Tao, S. S.; Huang, N.; Zhang, X. B.; Duan, J.; Makiura, R.; Maenosono, S. Heteroatom-doped carbon electrocatalysts derived from nanoporous two-dimensional covalent organic frameworks for oxygen reduction and hydrogen evolution. *ACS Appl. Nano Mater.* **2020**, 3, 5481-5488.
(67) Rao, P.; Wu, D.; Wang, T.-J.; Li, J.; Deng, P.; Chen, Q.; Shen, Y.; Chen, Y.; Tian, X. Single atomic cobalt electrocatalyst for efficient oxygen reduction reaction. *eScience* **2022**, doi.org/10.1016/j.esci.2022.05.004.
(68) Han, L.; Dong, S.; Wang, E. Transition-metal (Co, Ni, and Fe)-based electrocatalysts for the water oxidation reaction. *Adv. Mater.* **2016**, 28, 9266-9291.
(69) Fu, C. L.; Wang, Y.; Huang, J. H. Hybrid of quaternary layered double hydroxides and carbon nanotubes for oxygen evolution reaction. *Chin. J. Struct. Chem.* **2020**, 39, 1807-1816.
(70) Mou, Q.; Wang, X.; Xu, Z.; Zul, P.; Li, E.; Zhao, P.; Liu, X.; Li, H.; Cheng, G. A synergy establishment by metal-organic framework and carbon quantum dots to enhance electrochemical water oxidation. *Chin. Chem. Lett.* **2022**, 33, 562-566.
(71) Deng, B.; Liang, J.; Yue, L.; Li, T.; Liu, Q.; Liu, Y.; Gao, S.; Alshehri, A. A.; Alzahrani, K. A.; Luo, Y.; Sun, X. CoFe-LDH nanowire arrays on graphite felt: a high-performance oxygen evolution electrocatalyst in alkaline media. *Chin. Chem. Lett.* **2022**, 33, 890-892.
(72) Chen, K.; Mao, K.; Bai, Y.; Duan, D.; Chen, S.; Wang, C.; Zhang, N.; Long, R.; Wu, X.; Song, L.; Xiong, Y. Phosphate-induced interfacial electronic engineering in VPO_4-Ni_2P heterostructure for improved electrochemical water oxidation. *Chin. Chem. Lett.* **2022**, 33, 452-456.
(73) Lu, X. F.; Liao, P. Q.; Wang, J. W.; Wu, J. X.; Chen, X. W.; He, C. T.; Zhang, J. P.; Li, G. R.; Chen, X. M. An alkaline-stable, metal hydroxide mimicking metal-organic framework for efficient electrocatalytic oxygen evolution. *J. Am. Chem. Soc.* **2016**, 138, 8336-8339.
(74) Mondal, S.; Mohanty, B.; Nurhuda, M.; Dalapati, S.; Jana, R.; Addicoat, M.; Datta, A.; Jena, B. K.; Bhaumik, A. A thiadiazole-based covalent organic framework: a metal-free electrocatalyst toward oxygen evolution reaction. *ACS Catal.* **2020**, 10, 5623-5630.
(75) Yang, C.; Yang, Z.-D.; Dong, H.; Sun, N.; Lu, Y.; Zhang, F.-M.; Zhang, G. Theory-driven design and targeting synthesis of a highly-conjugated basal-plane 2D covalent organic framework for metal-free electrocatalytic OER. *ACS Energy Lett.* **2019**, 4, 2251-2258.
(76) Riha, S. C.; Klahr, B. M.; Tyo, E. C.; Seifert, S.; Vajda, S.; Pellin, M. J.; Hamann, T. W.; Martinson, A. B. F. Atomic layer deposition of a submonolayer catalyst for the enhanced photoelectrochemical performance of water oxidation with hematite. *ACS Nano* **2013**, 7, 2396-2405.
(77) Jia, H.; Sun, Z.; Jiang, D.; Du, P. Covalent cobalt porphyrin framework on multi-walled carbon nanotubes for efficient water oxidation at low overpotential. *Chem. Mater.* **2015**, 27, 4586-4593.
(78) Aiyappa, H. B.; Thote, J.; Shinde, D. B.; Banerjee, R.; Kurungot, S. Cobalt-modified covalent organic framework as a robust water oxidation electrocatalyst. *Chem. Mater.* **2016**, 28, 4375-4379.
(79) Mullangi, D.; Dhavale, V.; Shalini, S.; Nandi, S.; Collins, S.; Woo, T.; Kurungot, S.; Vaidhyanathan, R. Low-overpotential electrocatalytic water splitting with noble-metal-free nanoparticles supported in a sp^3 N-rich flexible COF. *Adv. Energy Mater.* **2016**, 6, 1600110.
(80) Nandi, S.; Singh, S. K.; Mullangi, D.; Illathvalappil, R.; George, L.; Vinod, C. P.; Kurungot, S.; Vaidhyanathan, R. Low band gap benzimidazole COF supported Ni_3N as highly active OER catalyst. *Adv. Energy Mater.* **2016**, 6, 1601189.
(81) Fan, X.; Kong, F.; Kong, A.; Chen, A.; Zhou, Z.; Shan, Y. Covalent porphyrin framework-derived Fe_2P@Fe_4N-coupled nanoparticles embedded in N-doped carbons as efficient trifunctional electrocatalysts. *ACS Appl. Mater. Interfaces* **2017**, 9, 32840-32850.
(82) Singh, A.; Roy, S.; Das, C.; Samanta, D.; Maji, T. K. Metallophthalocyanine-based redox active metal-organic conjugated microporous polymers for OER catalysis. *Chem. Commun.* **2018**, 54, 4465-4468.
(83) Zhuang, G.-l.; Gao, Y.-F.; Zhou, X.; Tao, X.-Y.; Luo, J.-M.; Gao, Y.-J.; Yan, Y.-l.; Gao, P.-Y.; Zhong, X.; Wang, J.-G. ZIF-67/COF-derived highly dispersed Co_3O_4/N-doped porous carbon with excellent performance for oxygen evolution reaction and Li-ion batteries. *Chem. Eng. J.* **2017**, 330, 1255-1264.
(84) Yang, W. G.; Gong, Z. W.; Chen, Y. N.; Chen, R. R.; Meng, D. L.; Cao, M. N. Nitrogen doped carbon as efficient catalyst toward oxygen reduction reaction. *Chin. J. Struct. Chem.* **2020**, 39, 287-293.
(85) Cui, Y. Q.; Xu, J. X.; Wang, M. L.; Guan, L. H. Surface oxidation of single-walled-carbon-nanotubes with enhanced oxygen electroreduction activity and selectivity. *Chin. J. Struct. Chem.* **2021**, 40, 533-539.
(86) Wang, K.; Pang, Y. Y.; Xie, H.; Sun, Y.; Chai, G. L. Synergistic effect of Ta_2O_5/F-C composites for effective electrosynthesis of hydrogen peroxide from O_2 reduction. *Chin. J. Struct. Chem.* **2021**, 40, 225-232.
(87) Song, Y.; Peng, Y.; Yao, S.; Zhang, P.; Wang, Y.; Gu, J.; Lu, T.; Zhang, Z. Co-POM@MOF-derivatives with trace cobalt content for highly efficient oxygen reduction. *Chin. Chem. Lett.* **2022**, 33, 1047-1050.
(88) Royuela, S.; Martinez-Perinan, E.; Arrieta, M. P.; Martinez, J. I.; Ramos, M. M.; Zamora, F.; Lorenzo, E.; Segura, J. L. Oxygen reduction using a metal-free naphthalene diimide-based covalent organic framework electrocatalyst. *Chem. Commun.* **2020**, 56, 1267-1270.
(89) Xiang, Z.; Cao, D.; Huang, L.; Shui, J.; Wang, M.; Dai, L. Nitrogen-doped holey graphitic carbon from 2D covalent organic polymers for oxygen reduction. *Adv. Mater.* **2014**, 26, 3315-3320.
(90) Zuo, Q.; Cheng, G.; Luo, W. A reduced graphene oxide/covalent cobalt porphyrin framework for efficient oxygen reduction reaction. *Dalton Trans.* **2017**, 46, 9344-9348.
(91) Xu, Q.; Tang, Y.; Zhang, X.; Oshima, Y.; Chen, Q.; Jiang, D. Template conversion of covalent organic frameworks into 2D conducting nanocarbons for catalyzing oxygen reduction reaction. *Adv. Mater.* **2018**, 30, 1706330.
(92) Liu, W.; Wang, C.; Zhang, L.; Pan, H.; Liu, W.; Chen, J.; Yang, D.;

Xiang, Y.; Wang, K.; Jiang, J.; Yao, X. Exfoliation of amorphous phthalocyanine conjugated polymers into ultrathin nanosheets for highly efficient oxygen reduction. *J. Mater. Chem. A* **2019**, 7, 3112-3119.

(93) Chai, D.; Min, X.; Harada, T.; Nakanishi, S.; Zhang, X. Covalent triazine framework anchored with atomically dispersed iron as an efficient catalyst for advanced oxygen reduction. *Colloids Surf. A* **2021**, 628, 127240.

(94) Wang, Y.; Batmunkh, M.; Mao, H.; Li, H.; Jia, B.; Wu, S.; Liu, D.; Song, X.; Sun, Y.; Ma, T. Low-overpotential electrochemical ammonia synthesis using BiOCl-modified 2D titanium carbide MXene. *Chin. Chem. Lett.* **2022**, 33, 394-398.

(95) Li, S.; Liang, J.; Wei, P.; Liu, Q.; Xie, L.; Luo, Y.; Sun, X. ITO@TiO_2 nanoarray: an efficient and robust nitrite reduction reaction electrocatalyst toward NH_3 production under ambient conditions. *eScience* **2022**, doi.org/10.1016/j.esci.2022.04.008.

(96) Hong, Q. S.; Li, T. Y.; Zheng, S. S.; Chen, H. B.; Chu, H. H.; Xu, K. D.; Li, S. N.; Mei, Z. W.; Zhao, Q. H.; Ren, W. J.; Zhao, W. G.; Pan, P. Tuning double layer structure of WO_3 nanobelt for promoting the electrochemical nitrogen reduction reaction in water. *Chin. J. Struct. Chem.* **2021**, 40, 519-526.

(97) Liu, S.; Wang, M.; Qian, T.; Ji, H.; Liu, J.; Yan, C. Facilitating nitrogen accessibility to boron-rich covalent organic frameworks via electrochemical excitation for efficient nitrogen fixation. *Nat. Commun.* **2019**, 10, 3898.

(98) Jiang, M.; Han, L.; Peng, P.; Hu, Y.; Xiong, Y.; Mi, C.; Tie, Z.; Xiang, Z.; Jin, Z. Quasi-phthalocyanine conjugated covalent organic frameworks with nitrogen-coordinated transition metal centers for high-efficiency electrocatalytic ammonia synthesis. *Nano Lett.* **2022**, 22, 372-379.

(99) Zhang, M. D.; Yi, J. D.; Huang, Y. B.; Cao, R. Covalent triazine frameworks-derived N,P dual-doped porous carbons for highly efficient electrochemical reduction of CO_2. *Chin. J. Struct. Chem.* **2021**, 40, 1213-1222.

(100) Wu, Q.; Xie, R. K.; Mao, M. J.; Chai, G. L.; Yi, J. D.; Zhao, S. S.; Huang, Y. B.; Cao, R. Integration of strong electron transporter tetrathiafulvalene into metalloporphyrin-based covalent organic framework for highly efficient electroreduction of CO_2. *ACS Energy Lett.* **2020**, 5, 1005-1012.

Received: 28 June, 2022
Accepted: July 18, 2022
Published online: July 29, 2022
Published: October 31, 2022

Cha Li received his B.S. degree from Yichun University in 2019 and M.S. degree from Tianjin Normal University in 2022. Now, he is pursuing his Ph.D. degree at Nankai University. His current research focuses on the applications of crystalline porous materials in energy catalysis and functional devices.

Zining Qiu received her B.S. degree from Gannan Normal University in 2021 and is currently pursuing her master's degree. Her current research focuses on the design and application of electrocatalyst for hydrogen evolution reaction.

Hongming Sun received his B.E. degree from Shandong University of Technology in 2012 and M.S. degree from Tianjin Polytechnic University in 2015. He then joined Professor Fangyi Cheng's group in the College of Chemistry at Nankai University and received his Ph.D. degree in 2018. Now, he works in the College of Chemistry at Tianjin Normal University. His research focuses on developing transition-metal-based materials for electrocatalytic hydrogen evolution, hydrogen oxidation, nitrogen reduction and oxygen evolution.

Yijie Yang received her bachelor degree from Nankai University in 2013 and PhD degree from Nanyang Technological University in 2018. She then joined College of Chemistry, Tianjin Normal University. Her current research interests focus on the design and fabrication of novel composite nanostructures and their application as electrocatalysts.

Cheng-Peng Li was born in Shanxi Province, China (1981). He received his BS (2003) and MS (2006) from Tianjin Normal University and subsequently his PhD from Tianjin University (2009). He then joined the faculty at Tianjin Normal University and is now a Professor of Chemistry. He has worked with Prof. Wuzong Zhou at University of St Andrews. His current research lies in porous crystalline materials (MOFs, COFs, and HOFs) and their applications in adsorption and catalysis.

DOI: 10.14102/j.cnki.0254-5861.2022-0162